MINERALOGICAL SOCIETY OF AMERICA, SPECIAL PAPER 1, 1963
INTERNATIONAL MINERALOGICAL ASSOCIATION, PAPERS, THIRD GENERAL MEETING

TRENDS AND AFFINITIES OF BASALTIC MAGMAS AND PYROXENES AS ILLUSTRATED ON THE DIOPSIDE—OLIVINE—SILICA DIAGRAM

D. S. COOMBS
Geology Department, University of Otago, Dunedin, New Zealand

ABSTRACT

The major normative components of basalts can be accommodated in the tetrahedra plagioclase—diopside—olivine—silica or plagioclase—diopside—olivine—nepheline. Average compositions of magma batches from basaltic provinces project from the plagioclase point as a broad band extending across the base of the tetrahedra. At one extreme are types in which an "indicator ratio"

$$\frac{Hy + 2Qz}{Hy + 2(Qz + Di)} = 0.65 - 0.85,$$

and from which early precipitation of hypersthene is common. Differentiation leads to granophyric products. Where the indicator ratio is less than 0.60—0.65 hypersthene, if present, tends to follow augite. Hypersthene is seldom found where the ratio is less than 0.50. For typical tholeiites, the indicator ratio is 0.65 ± 0.20. In the range 0.40 to 0.00 is a rather heterogeneous group including the high-alumina basalts of Medicine Lake Highlands as well as mildly alkaline suites such as Ascension Island, Easter Island and Réunion. The latter examples tend to show a pantelleritic differentiation trend. Averages for the more typical alkaline suites have normative nepheline instead of hypersthene and have trachytic and phonolitic associates. Analyses of pyroxenes from alkaline basalts contain normative Ne; those from tholeiites commonly contain normative Di, Ol, Hy. Separation of such pyroxenes from their parent magma in general accentuates the undersaturated or oversaturated nature of the magma with respect to the plagioclase—diopside—olivine plane. Consideration of crystallization trends allows the approximate location of a five-phase "point" (olivine, augite, hypersthene, plagioclase, liquid) and interpretation of reaction relationships. Clustering of analyses of typical tholeiites around this point suggests that they have originated as liquids coexisting with the four solid phases mentioned.

INTRODUCTION

Yoder and Tilley (1957) have recently emphasized the importance in basaltic petrogenesis of the relations described by Bowen (1914) in the system $CaMgSi_2O_6$-Mg_2SiO_4-SiO_2. For ordinary pressures, the olivine-pyroxene reaction relationship should be shown by those liquids which start their crystallization in that part of the forsterite field below and to the right of a line joining Mg_2SiO_4 to the point where the pyroxene-forsterite field boundary crosses the $MgSiO_3$-$CaMgSi_2O_6$ join (Fig. 1). Such liquids may be compared with simplified tholeiitic magmas. In contrast alkali basalt magmas do not show this reaction relationship and if they may be represented on this diagram at all, they may be compared with liquids that commence their crystallization in the wedge-shaped area to the left of the join referred to, that is near the forsterite-diposide side of the triangular diagram.

In spite of the fundamental significance to petrogenesis of relationships in this system, systematic attempts to plot appropriate rock compositions on a corresponding diagram do not appear to have been published.[1] Some of the relationships which are revealed by the use of such diagrams are explored in the present paper.

The diagrams here used may be regarded as projections from the plagioclase apex onto the bases of a plagioclase-ferroan diopside-olivine-silica tetrahedron, and of a corresponding plagioclase-nepheline-olivine-ferroan diopside tetrahedron for more strongly undersaturated compositions. Compositions are plotted in terms of molecular proportions of the normative components. In the case of common basaltic rocks virtually all constituents, except iron ores, are accommodated by the tetrahedra concerned. The projections are designed primarily to portray variation in silica saturation. Variations in iron/magnesium and alkali/lime ratios, effectively illustrated in certain other diagrams, are not revealed. An advantage sought by Murata (1960) in a proposed method for plotting basaltic rock analyses is achieved, namely that compositions of the major minerals are

[1] Since this was written Tilley (1961) has plotted Hawaiian basalts on diagrams of this sort, though he favours plots in weight per cent rather than molecular per cent as here employed.

clearly represented. Furthermore rock compositions are portrayed in a manner which with certain qualifications, directly reflects the crystallization history of the rock as has long been achieved in phase diagrams of synthetic systems and in plots of rocks whose compositions approach those of petrology's residua system $NaAlSiO_4$-$KAlSiO_4$-SiO_2.

ACKNOWLEDGMENTS

For some years the writer has used in his lecture courses diagrams of the type presented here. During late 1959 and 1960 he had the opportunity of discussing problems of basalt petrogenesis with many geologists including Drs. G. A. Chinner, I. D. Muir, K. J. Murata, S. R. Nockolds, D. H. Richter, Professors C. E. Tilley and O. F. Tuttle and Dr. H. S. Yoder. While he accepts full responsibility for the general approach and the opinions here expressed, the writer is conscious that the treatment has been greatly enriched through these discussions. Several of those mentioned critically read a manuscript of the present paper during late 1960, a number of additional data and minor changes having been incorporated since. The writer is particularly grateful to Professor E. F. Osborn for critical comments on the manuscript, to Professor Tilley and Dr. Muir for much interesting information and to Professor Tilley for the hospitality of the Department of Mineralogy and Petrology, Cambridge, where most of the manuscript was prepared, to the United States Educational Foundation for a Fulbright travel award and to the Pennsylvania State University

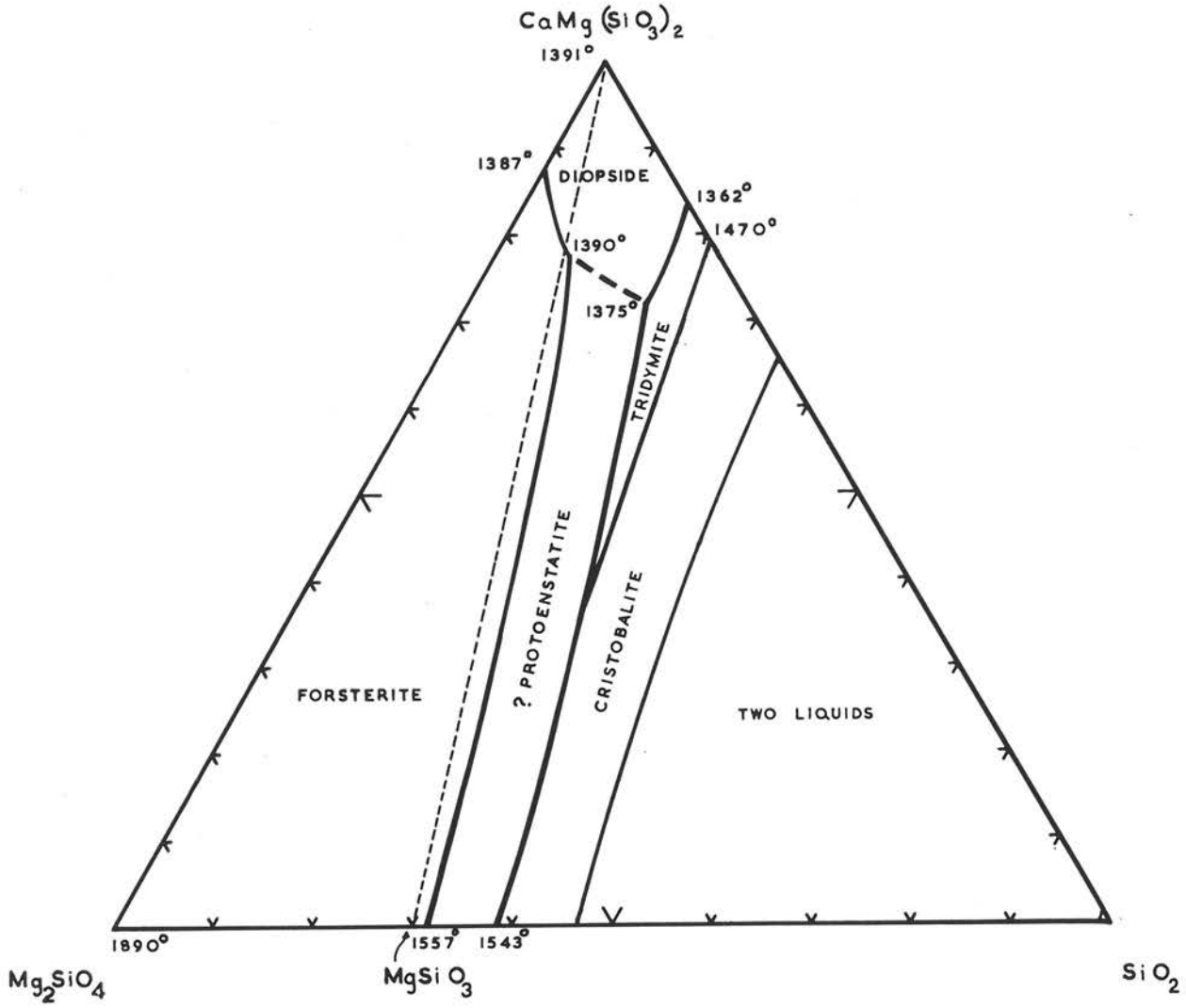

FIG. 1. The system $CaMgSi_2O_6$-Mg_2SiO_4-SiO_2, after Bowen (1914) and Osborn and Muan (1960).
Note added in proof: For revised diagram, see Schairer and Yoder (1962) *Carn. Inst. Wash. Year Book*, **61**, 76.

whose guest the writer was during the Spring Semester of 1960.

Effects of Added Components on Relations in the System $CaMgSi_2O_6$-Mg_2SiO_4-SiO_2

Probable relationships in the four-component system diopside-forsterite-anorthite-silica (Fig. 2), based on interpolation from the four bounding ternary systems, have been illustrated by Osborn and Tait (1952). Boyd and Schairer (1957) have subsequently demonstrated an immiscibility gap in the diopside-clinoenstatite series. This requires subdivision of the pyroxene field in the ternary system (Fig. 1) as indicated tentatively by Osborn and Muan (1960, Plate 2). The pyroxene volume in the quaternary system must also be subdivided into separate volumes for at least two pyroxenes. The anorthite volume forms a roof to those of forsterite, pyroxenes and the silica minerals. Disregarding the subdivision of the pyroxene volume, the projection of this "roof" from

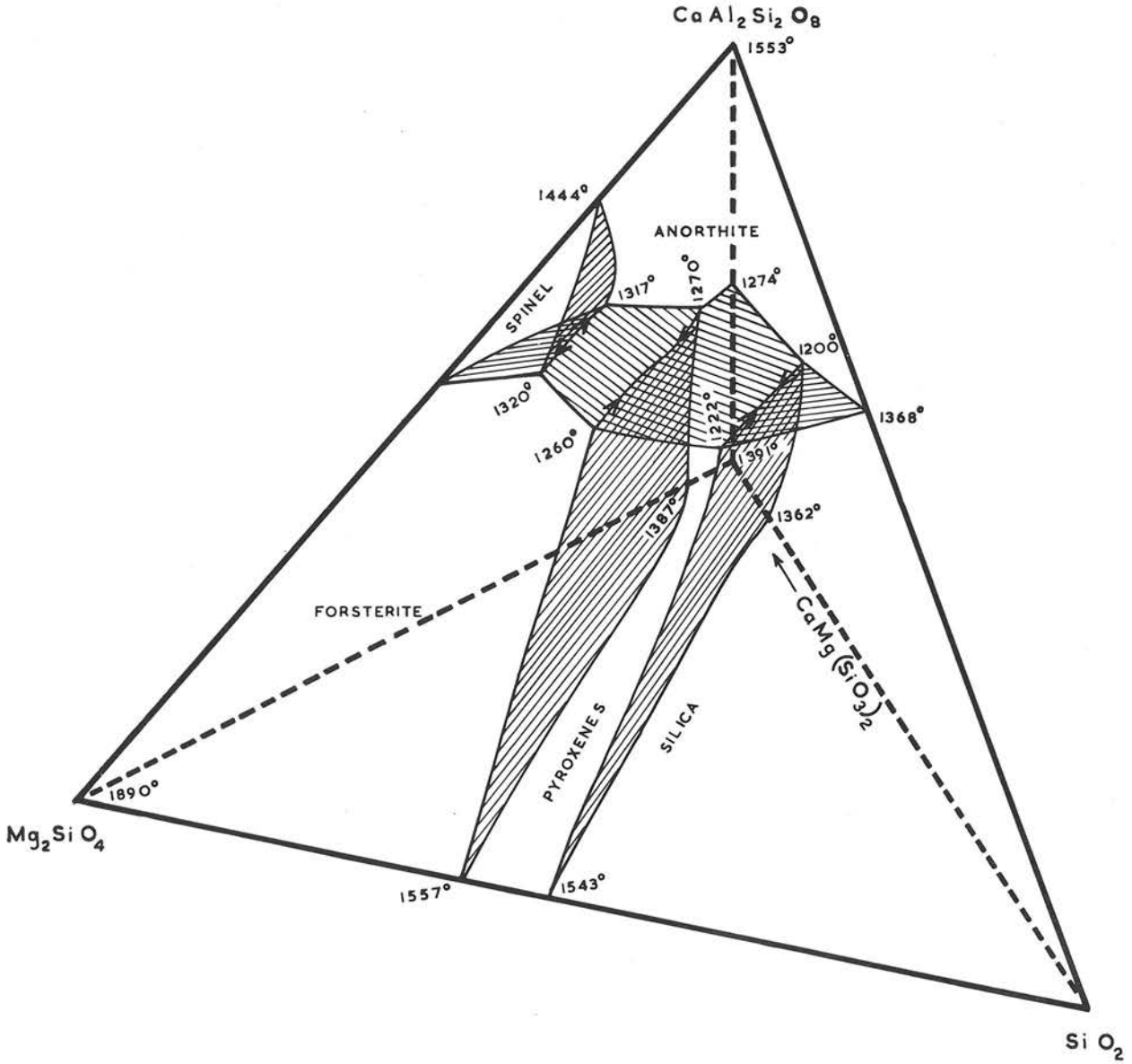

FIG. 2. Schematic representation of relations in the four component system $CaAl_2Si_2O_8$-$CaMgSi_2O_6$-Mg_2SiO_4-SiO_2 neglecting subdivision of the pyroxene volume (adapted from Osborn & Tait, 1952). The "floor" of the anorthite volume is shown shaded. It is crossed by three four-phase invariant lines: anorthite-spinel-forsterite-liquid, anorthite-forsterite-pyroxene-liquid, anorthite-pyroxene-silica-liquid, where it intersects other boundary surfaces, which are also shown shaded.

the anorthite point onto the base of the tetrahedron is shown schematically in Fig. 3, recast into molecular proportions for reasons discussed later. Following Osborn and Tait, temperature minima are indicated on the forsterite-pyroxene-anorthite-liquid and silica-pyroxene-anorthite-liquid univariant lines. It is probable that a two-pyroxene boundary surface will in fact intersect these univariant lines in five-phase invariant points that may also be the minima on the two boundary curves. Compositions and temperatures of the ternary and binary univariant points are indicated and the shape of the anorthite crystallization surface is shown schematically by contour lines indicating weight percentage anorthite, these being interpolated between the bounding ternary systems and the plane anorthite-enstatite-diopside studied by Hytönen and Schairer (1960).

From the position of the trace of the anorthite-metasilicate plane, it appears that the reaction relationships of Fig. 1 are unlikely to be upset by the presence of anorthite. In fact Andersen (1915) showed that in the plane anorthite-forsterite-silica the effect of anorthite is to extend the field in which the forsterite-enstatite reaction relationship prevails

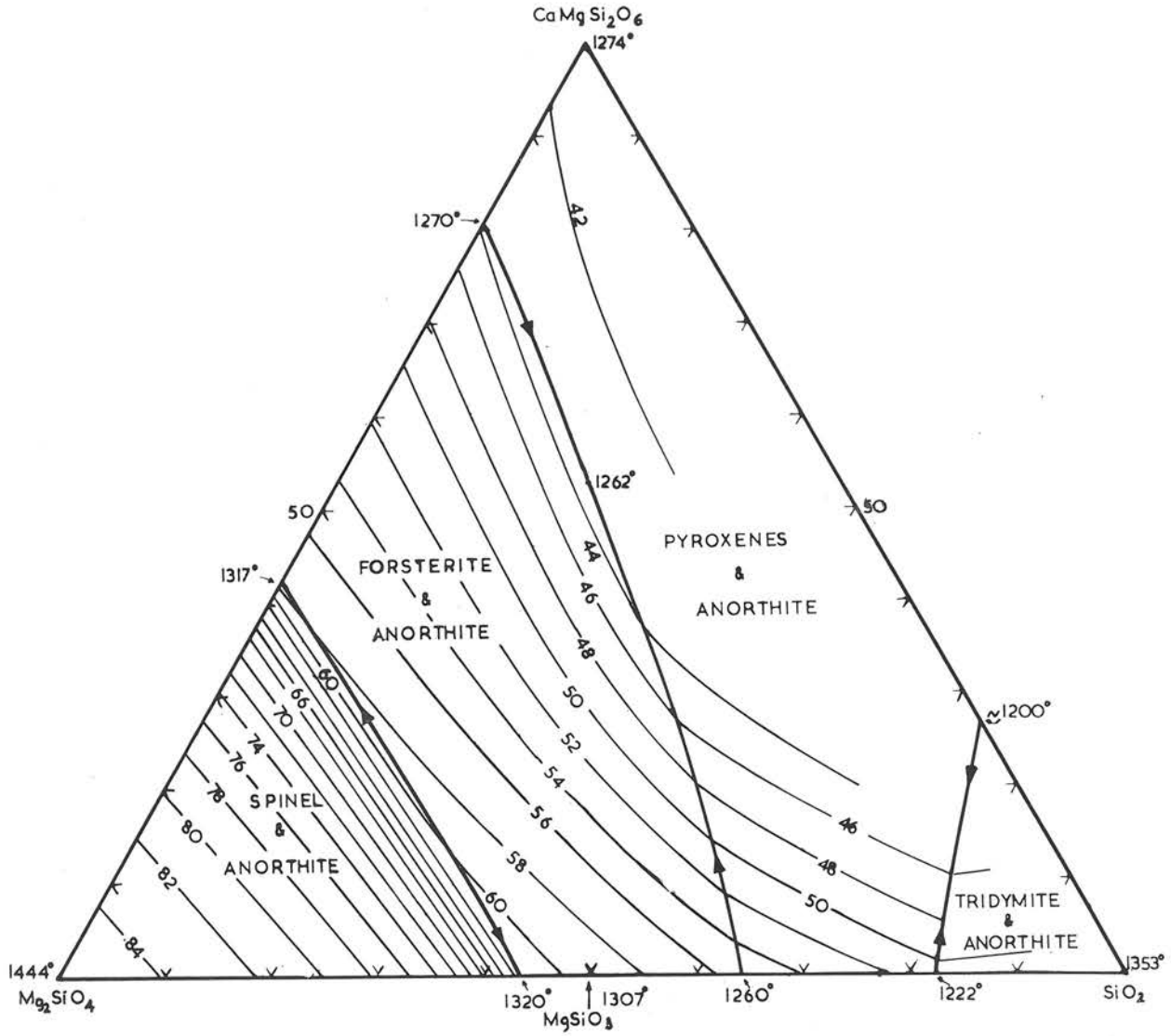

FIG. 3. Probable form of surface of the anorthite volume projected onto the base of the tetrahedron anorthite-diopside-forsterite-silica, disregarding subdivision of the pyroxene field; compositions in molecular per cent. Contours (marked in weight per cent) represent anorthite content of liquids existing on the three-phase surfaces as interpolated from boundary faces and the section enstatite-anorthite-diopside. Data from Andersen (1915), Osborn and Tait (1952), Hytönen and Schairer (1960).

However, if the interpretation of Osborn and Tait (1952) is correct, fractionation of liquids near the forsterite-diopside-anorthite plane should lead towards a minimum on the four-phase univariant line within the tetrahedron instead of to a eutectic or piercing point on the forsterite-diopside join as indicated by Bowen (1914) for the ternary system without anorthite. This fact could be crucial to the interpretation of the crystallization history of alkali olivine basalt magmas.

Presently published data do not allow the effect of albite to be evaluated in detail. Nevertheless behaviour in the planes enstatite-albite-diopside (Schairer and Morimoto, 1959) and albite-forsterite-silica (Schairer and Yoder, 1960) indicate that as albite replaces anorthite the plagioclase volume must shrink away from the diopside-forsterite-silica face, and that an olivine-"enstatite" reaction still prevails and may be further extended. The detailed effects of progressive substitution of iron for magnesium in the system are similarly uncertain, but as is well known from the work of Bowen and Schairer (1935) the olivine-pyroxene reaction relationship is destroyed by increasing iron content in the system MgO-FeO-SiO_2 so that ultimately fayalitic olivine can coexist stably with a silica mineral and a liquid whose composition is now on the olivine side of the metasilicate join. One may infer that in an infinite series of tetrahedra such as that in Fig. 2 in which iron progressively replaces magnesium and in which albite replaces anorthite, the position of the various three-phase surfaces and four-phase curves will progressively migrate. Increasing Fe/Mg ratios apparently reduce the range of compositions showing the olivine-"hypersthene" reaction relationship whereas increasing ratios of albite/anorthite may have the converse effect.

From the fact that typical basaltic liquids do coexist with the phases olivine, pyroxene and plagioclase feldspar and furthermore from the consistent pattern revealed when basaltic rocks and their pyroxenes are plotted in the tetrahedron, it may be inferred that crystallization relations for the common basaltic liquids have a general similarity in form to those of Fig. 2. It will be shown later that for common basalts the projected position of the four-phase curve olivine-pyroxene-plagioclase-liquid is remarkably close to its inferred position for the iron-free, albite-free system. Furthermore as normative feldspar constitutes about 50% by weight of total normative olivine or quartz plus pyroxenes plus feldspar in common basaltic rocks, it may also be inferred that the floor of a feldspar volume in a system plagioclase-ferroan diopside-olivine-silica must be in about the same position for basaltic compositions as it is in the system $CaAl_2Si_2O_8$-$CaMgSi_2O_6$-Mg_2SiO_4-SiO_2. Melts containing substantially more feldspar than this appear to commence crystallization in a plagioclase volume, as in the case of a hawaiite from Papalele Gulch, Mauna Kea, containing 61.2% normative feldspar (Yoder and Tilley, 1957). Melts containing lower plagioclase contents commonly commence crystallization in an olivine volume, apart from the more markedly oversaturated tholeiitic basalts in which the early crystallization products are pyroxenes and plagioclase to the exclusion of olivine.

Procedure

The metasilicate join, arbitrary indicator of silica saturation in igneous rocks, varies in its position on a weight per cent diopside-olivine-silica diagram as the Fe/Mg ratio is varied, and furthermore owing to the differing Fe/Mg ratios in crystals and liquid, liquids in the olivine field of a weight per cent diagram would follow a slightly curving instead of a straight course away from the olivine point, even though olivine may be the only phase separating. For clarity of interpretation rather than ease of plotting, diagrams based on molecular proportions are here adopted.

Compositions to the right of the metasilicate join in Fig. 3, conventionally considered as oversaturated, contain silica in the norm; those to the left are undersaturated and contain olivine. When silica is inadequate to satisfy diopside, olivine and feldspar, then nepheline and leucite appear in turn instead of hypersthene. It is therefore convenient to plot a second triangle $Ca(Mg,Fe)Si_2O_6$-$(NaAlSiO_4+KAlSi_2O_6)$-$(Mg,Fe)_2SiO_4$ alongside the first and having one edge in common. This may be considered as the base of a tetrahedron with feldspar at the apex and sharing a "critical plane of silica undersaturation" (Yoder and Tilley, 1960) with the plagioclase-ferroan diopside-olivine-silica tetrahedron. Compositions of rocks and minerals are thus plotted in this paper in terms of molecular proportions of $(NaAlSiO_4+KAlSi_2O_6)$: $Ca(Mg,Fe)Si_2O_6$: $(Mg,Fe)SiO_3$: $(Mg,Fe)_2SiO_4$: SiO_2 as computed during the calculation of the C.I.P.W. Norm, and recalculated to 100%. Well known tables for the calculation of the norm give molecular proportions (weight per cent divided by molecular weight) to three places of decimals. For some constituents this involves significantly less precision than is justified by the chemical analysis and furthermore the use of these three-figure tables invalidates the fourth

significant figure often cited in published norms. Revised molecular weights and a fourth figure have therefore been used during the calculation of norms for the present paper, and rounding to one place of decimals has been carried out at the end of the computation.

Effects of Analytical Error and Secondary Alteration

It is easy to demonstrate the amount and direction of scatter that is produced by given analytical errors in plots based on relative proportions of normative pyroxenes, olivine, silica or nepheline. Overestimation of alumina increases normative anorthite, olivine and nepheline or hypersthene at the expense of diopisde, whereas overestimation of lime or underestimation of P_2O_5 will result in overestimation of normative diopside. On account of the large amount of silica required to combine with alkalis in normative feldspar, errors in alkalis are of considerable importance, whereas normal errors in silica cause relatively minor disturbance. The effects of secondary oxidation and of analytical error in Fe_2O_3/FeO ratio are especially significant. It is well known that oxidation of ferrous iron tends to increase hypersthene in the norm at the expense of olivine (*e.g.* see Muir and Tilley, 1957, p. 251). As an example we may consider the effect of reducing the 3.14% Fe_2O_3 recorded for a certain basalt to 1.5% Fe_2O_3 with corresponding increase of FeO. In terms of relative molecular proportions of Qz, Di, Hy and Ol, Di remains constant at 35.4%, Hy drops from 62.6% to 56.4% and 8.2% Ol appears instead of 2.1% Qz. This type of difficulty is particularly perplexing in the case of alkaline basalts in which Fe_2O_3 and H_2O are commonly high, perhaps in part the result of an inherent property of alkali basalt magmas.

Two other types of secondary alteration are likely to be especially important. Serpentinization of olivine results in an increase of normative hypersthene with respect to olivine while alteration of glass to chlorite, palagonite or chlorophaeite appears to result commonly in a loss of lime, no doubt promoting the formation of calcite and zeolites in amygdaloidal horizons, and causing a serious decrease in normative diopside with respect to normative hypersthene and olivine in the massive rock. In the writer's view the many analyses of basaltic rocks in which such processes have been operative, cannot safely be regarded as precise representations of the composition of the original magma.

From this discussion and that of Fairbairn *et al.* (1951) it is obvious that analytical error and secondary alteration will produce an appreciable scatter on the Di-Ol-Qz and Di-Ol-Ne diagrams and for rocks such as some mugearites where total normative Di+Ol+Ne or Qz is 25% or less of the total rock, the plots will be of qualitative value only. The scatter of points which can be obtained by plotting the more aberrant individual analyses of the diabase W1 (Fairbairn *et al.*, 1951) emphasizes that too much significance must not be attached to individual analyses, but nevertheless it also appears that many generalized trends can be clearly portrayed. In fact batches of analyses of related unaltered rocks often show remarkably consistent patterns as in the case of the various phases of the 1921 and 1955 Kilauea eruptions (Fig. 8). In such cases the internal consistency can be appreciably enhanced by reducing Fe_2O_3 to some arbitrary value throughout the series, suggesting that even in very fresh rocks at least part of the Fe_2O_3 variation is due to secondary oxidation or to error in the determination of FeO.

A Series of Basaltic Magmas

It is obvious from the analyses that in typical tholeiitic basalts such as those from Tholey itself the ratio of normative hypersthene to diopside is in general rather high, whereas in those basalts having high alkali/silica ratios such as the alkali series of Hawaii (Tilley, 1950), hypersthene tends to be subordinate or absent. Such relationships are clearly relevant to the reaction relationship and the subsequent crystallization trend likely to be followed by a magma. Are these relationships capable of more systematic treatment?

In Table 1 the average compositions, norms and other data are given for basalts from a number of provinces, an attempt being made, in so far as the data allow, to ensure that the average represents a suite of rocks that is reasonably homogeneous in type, place and time. Except where special points are illustrated, the objective has been to obtain analyses representative of relatively voluminous batches of magma. The effects of averaging are both to smooth out analytical error and also to conceal real variation within the single volcano or province. Aspects of such intraprovincial variation are discussed later. The data are plotted on a Ne-Di-Ol-Qz diagram in Fig. 4.

Many of the averages have been taken from the literature; a few have been computed by the writer. In the latter case individual analyses showing more than 5% Fe_2O_3 or 5% H_2O have been discarded owing to the probability of secondary alteration and where published averages show more than 5% Fe_2O_3, these averages have also been rejected. Where the average

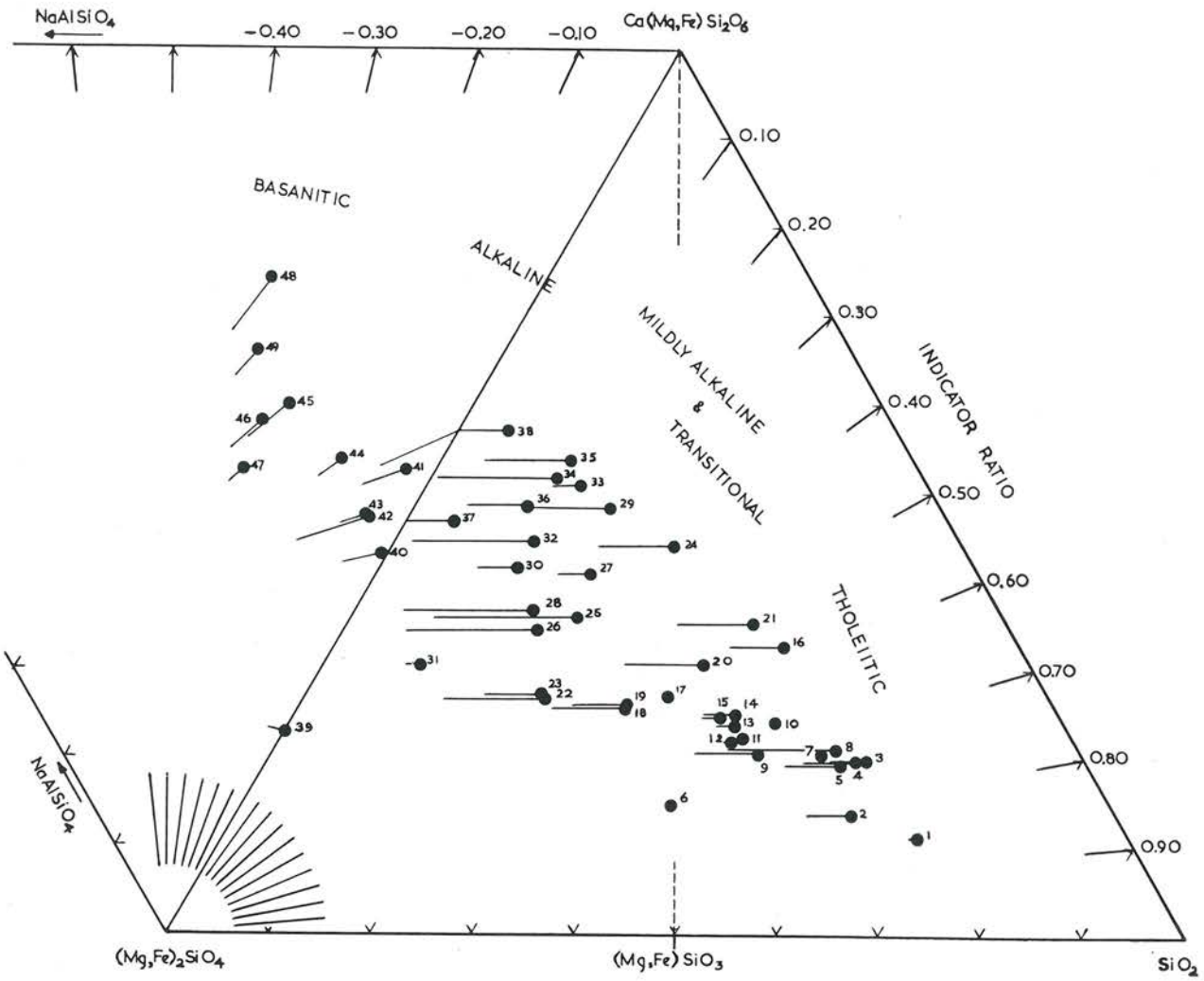

FIG. 4. Average compositions of basalts of various petrographic provinces plotted on a Ne-Di-Ol-Qz diagram (molecular proportions). See Table 1.

shows more than 1.5% Fe_2O_3, a line is drawn from the plotted point to where the analysis would plot if Fe_2O_3 were reduced to 1.5% and FeO increased correspondingly. This line gives an indication of the probable range of uncertainty in the plot in so far as oxidation effects are concerned.

Olivine is the first silicate phase to crystallize from perhaps the majority of basaltic magmas. In terms of the tetrahedral model of Fig. 2, crystallization commonly commences in the olivine volume and residual liquids must then move away from the point representing the olivine composition until they reach either the olivine-pyroxene or olivine-plagioclase boundary surface. They will then move along this towards an olivine-pyroxene-plagioclase-liquid four-phase curve, which as discussed above is not univariant but migrates with changing Fe/Mg and albite/anorthite ratios as well as with other variables in the natural system. The probability that basalts with high normative feldspar content may commence crystallization in the feldspar volume has already been referred to, but whether feldspar commences to crystallize early or late, so long as it carries neither an excess nor deficiency of silica, its separation does not affect the position of residual liquids on the projections here employed. It may be noted that many plagioclase analyses do in fact show a slight excess of silica. If this is real and not analytical, separation of plagioclase would thus tend to leave a residual liquid slightly impoverished in silica and to displace it slightly away from the silica corner of the projection. This possible effect will be neglected in the ensuing discussion.

No matter, then, at what stage plagioclase com-

KEY TO TABLE 1 AND FIG. 4

1. Peneplain Sill chilled margins, Ferrar dolerite, Victoria Land (Gunn, 1962).
2. Izu basalts, Japan, with $SiO_2 < 52\%$ (Kuno, 1950).
3. Columbia River basalt; Yakima basalt (Waters, 1961).
4. Izu basalts, Japan; aphyric types and groundmasses (Kuno, 1950).
5. Paleozoic tholeiites and quartz dolerites of north England and Scotland (Walker and Poldervaart, 1949).
6. Stillwater complex, border facies (Hess, 1960).
7. Ferrar dolerite chilled margins, moderate silica type, Victoria Land (Gunn, 1962).
8. Tholey tholeiites, Saar; two least oxidized analyses (Jung, 1958).
9. Koolau basalts, Oahu (Wentworth and Winchell, 1947).
10. Tasmanian dolerites; chilled phases (Edwards, 1942).
11. Karroo dolerites (Walker and Poldervaart, 1949).
12. Palisade diabase, chilled contacts (Walker, 1940).
13. Japanese "parental tholeiite" (Kuno, 1960).
14. Mauna Loa basalts, Hawaii (Macdonald, 1949a).
15. Columbia River basalts; late Yakima and early Ellensburg flows (Waters, 1961).
16. Deccan basalts (Sukheswala and Poldervaart, 1958).
17. Kilauea basalts, Hawaii (Macdonald, 1949a).
18. Greenstone flow, Lake Superior, weighted average (Cornwall, 1951).
19. Japanese "parental high-alumina basalt" (Kuno, 1960).
20. Columbia River (early) basalts; Picture Gorge basalt (Waters, 1961).
21. Non-porphyritic central magma type, Britain (Walker and Poldervaart, 1949).
22. Plateau basalts of Scotland (Green and Poldervaart, 1955).
23. Central Cascade Range, olivine basalts (Waters, 1961).
24. Western Australian Tertiary tholeiites (Edwards, 1938).
25. Ascension Island (Daly, 1925; Coombs and Harris, unpublished data).
26. Banks Peninsula, N.Z. (Benson, 1941).
27. Skjaldbreith shield volcano, Iceland (Tryggvason, 1943).
28. Tutuila, American Samoa (Daly, 1924).
29. Easter Island (least oxidized and hydrated; Bandy, 1937).
30. Galapagos Islands (Richardson, 1933).
31. Medicine Lake, California; high alumina basalt (Green and Poldervaart, 1955; Anderson, 1941).
32. Mauritius; Older Volcanic Series aphyric and microphyric basalts (Walker and Nicolaysen, 1954).
33. Réunion; basalt and dolerite, Volcan Actif (Walker and Nicolaysen, 1954).
34. Gambier Island (Mangareva), (Green and Poldervaart, 1955).
35. Réunion; basalts "des cônes interne et externe" (Lacroix, 1936, p. 192).
36. Réunion; Piton des Neiges (Lacroix, 1936, p. 211).
37. Mauna Kea, Hawaii; Hamakua volcanic series (Macdonald, 1949a).
38. Juan Fernandez; Mas-a-tierra (Green and Poldervaart, 1955).
39. Réunion; oceanites from Piton des Neiges (Lacroix, 1936, p. 214).
40. Alkali olivine basalts of Japan (Kuno, 1960).
41. Hualalai basaltic rocks, Hawaii (Macdonald, 1949a).
42. St. Helena (Daly, 1927).
43. Society Islands; Bora-Bora and neighbourhood (Lacroix, 1927).
44. Mauritius; late younger series basalts and dolerites (Walker and Nicolaysen, 1954).
45. Rungwe, East Africa; basaltic lavas excluding melanephelinites (Harkin, 1960).
46. East Otago, N.Z.; peripheral subprovince weighted average (Benson, 1942).
47. Auckland city basanitic basalts (Searle, 1960).
48. Tahiti basanitoid (Williams, 1933).
49. Honolulu series basanites (Winchell, 1947).

---

mences to crystallize, most basaltic liquids should appear to move radially away from the olivine composition on the Di-Ol-Qz or Ne-Di-Ol projection until they reach the projection of an olivine-pyroxene field boundary. The point at which this occurs is indicated by a radial line drawn from the olivine point through the projected liquid composition. For compositions on the high-silica side of the critical plane of silica undersaturation this radial may be defined by its intercept Qz/(Qz+Di) on the Qz-Di side of the Di-Ol-Qz diagram (Fig. 4). For any point lying within the triangle Di-Ol-Qz this intercept is given by the ratio

$$\frac{\text{Hy} + 2\text{Qz}}{\text{Hy} + 2(\text{Qz} + \text{Di})}$$

in molecular proportions. This ratio is here referred to as the *indicator ratio* (I.R.) since it indicates the projected course of any liquid from which olivine or olivine and plagioclase are the only phases crystallizing (*cf.* Fig. 8). Where Qz is absent from the norm, as in the presence of normative Ol, the ratio simplifies to

$$\frac{\text{Hy}}{\text{Hy} + 2\text{Di}}.$$

The indicator ratio is related to the silica-saturation expected for liquids as they reach the olivine-pyroxene field boundary. For compositions so deficient in silica as to contain normative nepheline, the indicator ratio may be considered to be negative and may be defined as

$$\frac{\text{NaAlSiO}_4}{\text{NaAlSiO}_4 + \text{Ca(Mg, Fe)Si}_2\text{O}_6}$$

in molecular proportions. Provision could also be made for normative leucite, if present.

It is instructive to consider various basaltic provinces in order of decreasing indicator ratio (Fig. 4),

TABLE 1. AVERAGED COMPOSITIONS FOR SOME BASALTIC SUITES

	1	2	3	4	5	6	7	8	9	10	11	12	13	14	15	16	17	18	19	20	21	22	23	24
No. of analyses	2	9	8	11	32	1	3	2	10	6	43	4	3	14	4	10	24	17	11	16	11	9	13	3
SiO_2	55.68	50.60	53.8	52.3	51.6	50.68	53.57	52.35	50.45	52.65	52.5	52.2	49.78	50.42	50.0	50.56	49.80	47.84	50.19	49.3	51.6	46.9	49.79	50.39
TiO_2	0.80	0.86	2.0	1.1	2.7	0.45	0.67	1.09	2.33	0.58	1.0	1.3	0.68	2.97	3.2	2.78	2.68	1.53	0.75	1.6	1.6	2.4	1.71	0.96
Al_2O_3	15.98	19.52	13.9	14.5	15.0	17.64	15.71	17.63	14.94	16.23	15.4	15.4	15.69	11.62	13.5	12.79	12.42	16.98	17.58	15.6	14.3	15.4	16.74	14.80
Fe_2O_3	1.81	2.82	2.6	3.8	3.4	0.26	1.25	4.21	3.38	0.51	1.2	1.6	2.73	2.71	1.9	3.23	1.53	3.18	2.84	3.5	3.5	3.9	2.65	3.38
FeO	8.01	7.21	9.3	10.2	9.6	9.88	7.87	4.23	7.55	8.21	9.3	8.7	9.20	9.07	12.5	11.28	9.91	7.92	7.19	7.8	9.2	9.8	7.82	8.31
MnO	0.17	0.17	0.2	0.3	0.2	0.15	0.17	0.15	0.08	0.15	0.2	0.1	0.35	0.10	0.25	0.22	0.13	0.17	0.25	0.2	0.3	0.3	0.17	0.20
MgO	4.17	4.49	4.1	5.1	4.9	7.71	6.36	5.42	7.67	6.64	7.1	7.3	7.79	10.11	4.4	5.40	10.31	6.73	7.39	6.5	5.3	8.4	7.16	6.03
CaO	8.42	11.04	7.9	10.0	8.9	10.47	10.63	9.13	9.17	11.34	10.3	10.0	11.93	9.74	8.3	10.29	10.32	10.01	10.50	10.3	10.1	9.6	9.07	10.93
Na_2O	2.34	1.94	3.0	2.1	2.4	1.87	1.85	3.02	2.84	1.58	2.1	2.4	1.21	2.09	2.9	2.55	1.96	2.63	2.75	2.7	2.8	2.5	3.32	2.93
K_2O	1.12	0.31	1.5	0.4	1.1	0.24	0.82	1.27	0.35	0.90	0.8	0.8	0.29	0.39	1.4	0.59	0.45	0.48	0.40	0.5	1.1	0.6	0.82	0.57
P_2O_5	0.10	0.10	0.4	0.2	0.2	0.09	0.08	0.21	0.27	0.01	0.1	0.2	0.07	0.27	0.7	0.31	0.29	0.18	0.14	0.3	0.3	0.2	0.31	0.04
H_2O	1.55	0.85	1.2	—	—	0.48	1.10	1.56	0.96	1.33	—	—	—	—	0.9	—	—	2.23	—	1.8	—	—	0.41	1.70
Others	—	—	—	—	—	0.04	—	0.04	0.12	—	—	—	0.29	—	0.09	—	—	0.12	—	0.04	—	—	0.02	0.02
Total	100.15	99.91	99.9	100.0	100.0	99.96	100.08	100.31	100.11	100.13	100.0	100.0	100.01	99.49	100.04	100.00	99.80	100.00	99.98	100.14	100.1	100.0	99.99	100.26
Norms (weight per cent)																								
qz	10.7	5.9	6.9	7.8	6.0	—	6.2	4.4	2.8	4.2	2.6	2.0	2.9	2.7	1.3	3.8	—	—	—	0.8	2.3	—	—	—
or	6.6	1.8	8.9	2.2	6.7	1.4	4.8	7.5	2.1	5.3	4.5	4.5	1.7	2.3	8.4	3.5	2.7	2.8	2.3	2.8	6.7	3.3	4.8	3.4
ab	19.8	16.4	25.2	17.8	20.4	15.8	15.6	25.5	23.5	13.4	17.8	20.5	10.2	17.7	24.7	21.6	16.6	22.2	23.3	23.1	23.6	21.0	28.1	24.8
ne	—	—	—	—	—	—	—	—	—	—	—	—	—	—	—	—	—	—	—	—	—	—	—	—
an	29.8	43.7	20.0	28.9	26.7	39.0	32.2	30.8	27.3	34.6	30.3	28.9	36.5	21.2	19.5	21.7	23.8	33.1	34.5	29.8	23.1	29.2	28.4	25.5
di wo	4.8	4.4	7.0	8.2	6.7	5.4	8.4	5.5	7.0	9.0	8.5	7.9	9.6	10.7	7.3	11.4	10.8	6.5	7.0	8.6	10.6	7.2	6.2	11.9
di en	2.2	2.3	3.2	3.8	3.5	2.7	4.5	4.1	4.6	4.7	4.5	4.4	5.3	7.1	2.9	5.5	6.8	3.9	4.3	5.2	5.4	4.4	3.8	6.5
di fs	2.6	2.0	3.7	4.4	3.1	2.5	3.6	0.9	1.8	4.0	3.7	3.2	3.9	2.7	4.5	5.7	3.3	2.2	2.3	2.9	4.9	2.4	2.0	4.9
hy en	8.2	8.9	7.0	8.9	8.7	16.1	11.3	9.4	14.4	11.8	13.1	13.8	14.1	18.0	8.0	7.9	18.1	9.7	10.8	10.9	7.7	7.9	6.5	8.2
hy fs	9.7	7.8	8.3	9.9	7.7	14.6	9.0	1.9	5.5	10.0	11.0	9.5	10.3	7.0	12.1	8.2	9.0	5.6	5.9	6.3	7.0	4.2	3.5	6.1
ol fo	—	—	—	—	—	0.3	—	—	—	—	—	—	—	—	—	—	0.5	2.2	2.4	—	—	6.1	5.3	0.2
ol fa	—	—	—	—	—	0.3	—	—	—	—	—	—	—	—	—	—	0.3	1.4	1.4	—	—	3.7	3.2	0.2
il	1.5	1.6	3.8	2.1	5.2	0.9	1.3	2.1	4.4	1.1	2.0	2.4	1.3	5.6	6.0	5.3	5.1	2.9	1.4	3.0	3.0	4.6	3.3	1.8
mt	2.6	4.1	3.7	5.6	4.9	0.4	1.8	6.1	5.0	0.7	1.9	2.3	4.0	3.9	2.8	4.7	2.2	4.6	4.1	5.1	5.1	5.6	3.8	4.9
ap	0.2	0.2	0.9	0.3	0.4	0.2	0.2	0.5	0.6	0.0	0.2	0.6	0.2	0.6	1.5	0.7	0.6	0.4	0.3	0.6	0.6	0.4	0.7	0.1
Others	1.5	0.9	1.2	—	—	0.5	1.1	1.6	1.1	1.3	—	—	—	—	1.0	—	—	2.4	—	1.8	—	—	0.4	1.7
Total	100.2	100.0	99.8	99.9	100.0	100.1	100.0	100.3	100.1	100.1	100.1	100.0	100.0	99.5	100.0	100.0	99.8	99.9	100.0	100.0	100.0	100.0	100.0	100.2
Molecular porportions $NaAlSiO_4$: $Ca(Mg, Fe)Si_2O_6$: $(Mg, Fe)SiO_3$: $(Mg, Fe)_2SiO_4$: SiO_2 (recalculated to 100%)																								
$NaAlSiO_4$	—	—	—	—	—	—	—	—	—	—	—	—	—	—	—	—	—	—	—	—	—	—	—	—
$Ca(Mg, Fe)Si_2O_6$	11.0	13.4	19.5	19.5	19.1	14.5	20.2	20.8	20.5	22.9	22.1	21.8	23.7	24.9	24.4	32.4	26.7	25.5	25.6	30.3	35.0	26.6	26.9	43.9
$(Mg, Fe)SiO_3$	41.5	52.2	43.3	44.8	47.9	84.5	50.8	47.1	63.6	56.7	64.6	67.2	62.6	63.1	67.0	46.5	71.8	64.1	64.3	64.4	50.0	47.2	46.3	55.1
$(mg, Fe)_2SiO_4$	—	—	—	—	—	1.0	—	—	—	—	—	—	—	—	—	—	1.5	10.4	10.1	—	—	26.2	26.8	1.0
SiO_2	47.5	34.4	37.2	35.7	33.0	—	29.0	32.1	15.9	20.5	13.3	10.9	13.7	12.0	8.6	21.1	—	—	—	5.3	15.0	—	—	—
Molecular proportions of Fe^{3+} reduced to Fe^{2+} to leave 1.50% Fe_2O_3																								
$NaAlSiO_4$	—	—	—	—	—	—	—	—	—	—	—	—	—	—	—	—	—	—	—	—	—	—	—	—
$Ca(Mg, Fe)Si_2O_6$	11.0	13.4	19.5	19.5	19.1	—	—	20.8	20.5	—	—	21.8	23.7	24.9	24.4	32.4	—	25.5	25.6	30.3	35.0	26.6	26.9	43.9
$(Mg, Fe)SiO_3$	43.0	61.0	50.2	55.5	59.8	—	—	69.4	75.7	—	—	68.2	69.2	69.8	70.5	57.2	—	49.6	53.7	59.1	65.0	27.9	35.4	39.9
$(Mg, Fe)_2SiO_4$	—	—	—	—	—	—	—	—	—	—	—	—	—	—	—	—	—	24.9	20.7	10.7	—	45.5	37.7	16.2
SiO_2	46.0	25.6	30.3	25.0	21.1	—	—	9.8	3.8	—	—	10.0	7.1	5.3	5.1	10.4	—	—	—	—	0.0	—	—	—
Indicator Ratio																								
Unadjusted	0.86	0.82	0.75	0.75	0.75	0.74	0.73	0.73	0.70	0.68	0.67	0.67	0.66	0.64	0.63	0.58	0.57	0.56	0.56	0.55	0.53	0.47	0.46	0.39
For Fe_2O_3=1.5%	0.86	0.81	0.74	0.73	0.73	—	—	0.68	0.67	—	—	0.67	0.64	0.62	0.62	0.55	—	0.49	0.52	0.49	0.48	0.34	0.40	0.31

TABLE 1. AVERAGED COMPOSITIONS FOR SOME BASALTIC SUITES—*Continued*

	25	26	27	28	29	30	31	32	33	34	35	36	37	38	39	40	41	42	43	44	45	46	47	48	49
No. of analyses	6	14	7	5	5	6	7	5	23	5	7	5	5	3	3	7	6	4	4	6	11	19	13	13	3
SiO_2	49.65	49.14	47.56	48.44	48.12	47.61	48.4	47.0	48.4	46.96	47.24	47.12	47.17	46.62	44.04	48.11	47.18	47.62	47.05	45.8	44.7	46.16	44.80	44.26	43.98
TiO_2	2.86	3.17	2.00	4.29	3.66	2.35	0.9	3.5	2.9	2.46	3.17	3.16	2.43	3.47	1.92	1.72	2.79	3.57	2.42	2.5	2.0	2.45	1.96	3.46	2.73
Al_2O_3	16.41	15.71	14.65	13.27	15.02	16.68	19.2	14.5	13.9	14.76	14.23	14.94	14.14	15.41	7.64	15.55	14.64	16.27	13.17	14.9	15.7	15.32	13.86	14.30	13.49
Fe_2O_3	3.71	3.64	2.35	4.06	2.93	2.31	1.8	4.0	2.3	3.68	3.30	2.73	3.05	4.57	3.05	2.99	3.17	3.87	2.67	3.0	4.1	3.50	2.91	4.61	3.53
FeO	7.38	8.17	9.92	8.27	9.79	8.80	7.3	9.0	9.2	7.68	8.76	9.34	8.81	7.66	9.45	7.19	9.00	8.17	8.76	9.9	8.5	9.67	9.63	7.79	8.79
MnO	0.23	0.15	0.24	0.15	0.14	0.22	0.1	0.2	0.1	0.16	0.13	0.11	0.12	0.19	0.11	0.16	0.09	0.11	0.15	0.2	0.1	0.21	0.17	0.21	0.10
MgO	5.08	6.03	8.53	8.21	4.42	6.89	8.0	7.5	7.8	8.12	7.16	6.63	9.23	6.73	22.78	9.31	8.19	6.33	10.65	8.8	8.4	7.25	11.07	8.34	10.19
CaO	8.43	8.38	12.59	7.72	9.45	11.26	11.2	10.1	11.9	11.94	11.15	10.42	10.96	10.49	7.22	10.43	10.70	8.65	9.99	11.1	11.6	9.58	10.16	11.26	11.11
Na_2O	3.81	3.69	1.78	3.47	3.48	2.66	2.7	2.7	2.3	2.31	2.51	2.65	2.54	2.98	1.64	2.85	3.04	3.82	2.63	2.9	2.9	3.74	3.19	3.48	3.49
K_2O	1.48	1.39	0.32	1.55	0.97	0.51	0.3	1.1	0.9	0.65	0.93	1.07	0.78	0.96	0.53	1.13	0.80	1.14	1.37	0.6	1.2	1.34	1.09	1.59	0.99
P_2O_5	0.68	0.73	0.20	0.57	0.30	0.26	0.1	0.4	0.3	0.22	0.15	0.19	0.38	0.30	0.07	0.56	0.49	0.45	0.33	0.3	0.8	0.65	0.55	0.70	0.54
H_2O	0.69	—	—	—	1.57	0.43	—	—	—	1.05	1.44	2.03	0.64	0.61	1.88	—	0.42	—	0.69	—	—	—	0.73	—	0.84
Others	—	—	—	—	0.16	—	—	—	—	—	—	—	0.05	—	—	—	—	—	0.04	—	—	0.20	—	—	0.29
Total	100.41	100.20	100.14	100.00	100.01	99.98	100.0	100.0	100.0	99.99	100.17	100.39	100.30	99.99	100.33	100.00	100.51	100.00	99.92	100.0	100.0	100.07	100.12	100.00	100.07
Norms (weight per cent)																									
qz	—	—	—	—	—	—	—	—	—	—	—	—	—	—	—	—	—	—	—	—	—	—	—	—	—
or	8.7	8.2	1.9	9.2	5.7	3.0	1.8	6.5	5.3	3.8	5.5	6.4	4.6	5.7	3.1	6.7	4.7	6.7	8.1	3.6	7.1	7.9	6.5	9.4	5.8
ab	32.2	31.2	15.0	29.4	29.4	22.5	22.9	22.9	19.5	19.6	21.2	22.4	21.5	25.2	13.9	23.8	24.2	30.8	19.6	18.6	13.6	20.4	13.0	11.7	11.0
ne	—	—	—	—	—	—	—	—	—	—	—	—	—	—	—	0.2	0.8	0.8	1.4	3.2	5.9	6.1	7.6	9.6	10.1
an	23.4	22.2	31.0	16.0	22.5	32.1	39.4	24.2	24.9	28.0	24.8	25.7	24.9	25.8	11.9	26.3	23.9	23.9	20.1	25.8	26.3	21.1	20.3	18.7	18.2
di wo	6.0	6.3	12.6	7.9	9.1	9.2	6.5	9.8	13.5	12.4	12.4	10.4	11.5	10.1	9.8	9.2	11.0	6.8	11.4	11.5	11.1	9.6	11.2	13.7	14.1
di en	3.8	4.0	7.4	5.7	4.7	5.4	4.0	6.5	8.3	8.4	7.9	6.2	7.5	7.2	7.3	6.3	7.0	4.5	7.7	7.0	7.2	5.6	7.2	9.9	9.6
di fs	1.9	1.9	4.7	1.4	4.2	3.4	2.1	2.7	4.4	3.1	3.7	3.7	3.2	2.1	1.5	2.2	3.3	1.8	2.9	3.8	3.1	3.5	3.3	2.5	3.4
hy en	4.7	4.5	7.6	5.6	3.8	3.6	2.6	4.1	5.1	4.1	3.8	2.9	1.6	1.2	0.2	—	—	—	—	—	—	—	—	—	—
hy fs	2.3	2.0	4.8	1.4	3.4	2.2	1.4	1.7	2.7	1.5	1.8	1.7	0.7	0.4	0.0	—	—	—	—	—	—	—	—	—	—
ol fo	2.9	4.6	4.4	6.4	1.8	5.7	9.3	5.7	4.3	5.4	4.3	5.2	9.8	5.9	34.5	11.9	9.4	7.9	13.2	10.5	9.6	8.7	14.3	7.6	11.0
ol fa	1.6	2.4	3.1	1.7	1.7	4.0	5.5	2.7	2.5	2.1	2.2	3.4	4.6	1.9	8.0	4.6	4.8	3.4	5.5	6.3	4.6	6.0	7.0	2.1	4.3
il	5.4	6.0	3.8	8.1	6.9	4.5	1.7	6.6	5.5	4.7	6.0	6.0	4.6	6.6	3.6	3.3	5.3	6.7	4.6	4.7	3.8	4.6	3.7	6.6	5.2
mt	5.4	5.3	3.4	5.9	4.3	3.4	2.6	5.8	3.3	5.3	4.8	4.0	4.4	6.6	4.4	4.3	4.6	5.6	3.9	4.4	6.0	5.1	4.2	6.7	5.1
ap	1.5	1.6	0.4	1.2	0.9	0.6	0.2	0.9	0.7	0.5	0.3	0.4	0.8	0.7	0.2	1.2	1.1	1.0	0.7	0.7	1.8	1.4	1.2	1.6	1.2
Others	0.7	—	—	—	1.7	0.4	—	—	—	1.1	1.4	2.0	0.7	0.6	1.9	—	0.4	—	0.7	—	—	0.1	0.7	—	1.1
Total	100.5	100.2	100.1	99.9	100.1	100.0	100.0	100.1	100.0	100.0	100.1	100.4	100.4	100.0	100.3	100.0	100.5	99.9	99.8	100.1	100.1	100.1	100.2	100.1	100.1
Molecular Proportions																									
$NaAlSiO_4$	—	—	—	—	—	—	—	—	—	—	—	—	—	—	—	0.6	3.0	4.0	4.4	10.0	18.3	19.9	18.7	27.1	24.3
$Ca(Mg, Fe)Si_2O_6$	35.8	34.2	40.6	36.3	48.1	41.3	30.2	44.2	50.6	51.5	53.4	48.2	46.7	56.9	22.8	42.4	49.7	43.1	42.9	43.6	41.7	38.0	33.8	47.1	41.6
$(Mg, Fe)SiO_3$	44.3	36.1	42.2	35.0	38.9	27.4	19.5	27.9	30.9	25.2	25.7	22.7	9.7	9.8	0.4	—	—	—	—	—	—	—	—	—	—
$(Mg, Fe)_2SiO_4$	19.9	27.7	17.2	28.8	13.0	31.3	50.3	27.9	18.5	23.3	20.9	29.1	43.6	33.3	76.8	57.0	47.3	52.9	52.7	46.4	40.0	42.1	47.5	25.8	34.1
SiO_2	—	—	—	—	—	—	—	—	—	—	—	—	—	—	—	—	—	—	—	—	—	—	—	—	—
Molecular Proportions if Fe^3 reduced to Fe^2 to leave 1.50% Fe_2O_3																									
$NaAlSiO_4$	—	—	—	—	—	—	—	—	—	—	—	—	1.0	5.9	1.8	4.0	6.4	9.8	6.4	11.2	20.4	21.4	19.5	28.0	25.1
$Ca(Mg, Fe)Si_2O_6$	35.8	34.2	40.6	36.3	48.1	41.3	30.2	44.2	50.6	51.5	53.4	48.2	45.4	47.0	21.6	38.1	44.2	34.6	40.0	40.2	35.9	33.5	31.7	40.1	37.9
$(Mg, Fe)SiO_3$	16.3	12.8	36.2	9.4	22.3	19.4	16.4	3.5	24.4	0.8	8.7	10.2	—	—	—	—	—	—	—	—	—	—	—	—	—
$(Mg, Fe)_2SiO_4$	47.9	53.0	23.1	54.3	29.6	39.2	53.3	52.3	25.0	47.8	37.9	41.6	53.6	47.1	76.6	57.9	49.3	55.6	53.7	48.6	43.7	45.1	48.8	31.9	37.0
SiO_2	—	—	—	—	—	—	—	—	—	—	—	—	—	—	—	—	—	—	—	—	—	—	—	—	—
Indicator Ratio																									
Unadjusted	0.38	0.36	0.34	0.33	0.29	0.25	0.24	0.24	0.23	0.20	0.19	0.19	0.09	0.08	0.01	−0.01	−0.06	−0.09	−0.09	−0.19	−0.31	−0.34	−0.36	−0.37	−0.37
For Fe_2O_3=1.5%	0.19	0.16	0.31	0.12	0.19	0.19	0.21	0.04	0.19	0.01	0.08	0.10	−0.02	−0.11	−0.08	−0.10	−0.13	−0.22	−0.14	−0.22	−0.36	−0.39	−0.38	−0.41	−0.40

Indicator ratio 0.85 to 0.65. Magma batches for which this ratio exceeds 0.65 include the Izu basalts of Japan (2, 4), Ferrar dolerites of Antarctica (1, 7), the Yakima basalts of the Columbia River group (3), British Paleozoic tholeiites and quartz-tholeiites (5), Stillwater border facies (6), the type tholeiites from Tholey, Saar (8), Koolau Series of Oahu (9), the Tasmania (10), Karroo (11) and Palisade (12) dolerites and Kuno's average Japanese tholeiite (13). In these provinces, except in the somewhat altered rocks of Tholey where hypersthene is rare (Jung, 1958), and the Columbia River basalts, hypersthene characteristically appears early. It is soon joined by clinopyroxene, although this situation may occasionally be reversed, and olivine shows the reaction relationship to hypersthene or pigeonite. Differentiation in place leads to granophyric residua as demonstrated in many quartz dolerite sills and in the Palolo quartz dolerite of the Koolau Series, Oahu (Kuno *et al.*, 1957).

Indicator ratio 0.65 to 0.50. In the range of indicator ratio from 0.65 to 0.50 are the average basalt from Mauna Loa (14), the late Yakima flows of Columbia River (15), Deccan (16), Kilauea (17), the Keweenawan Greenstone flow of Lake Michigan (18), Kuno's average Japanese high-alumina basalt (19), Picture Gorge basalts (early Columbia River, 20) and the non-porphyritic central magma type of Scotland (21). In the case of Kilauea, olivine occurs as phenocrysts and occasionally in the groundmass, usually without any conspicuous reaction relationship (Macdonald, 1949a). Throughout the group hypersthene appears to be distinctly less common than in the group with I.R. 0.85 to 0.65 above. For example the pyroxenes reported by West (1958) and Naidu (1960) for the Deccan basalts of central India (I.R.=0.58) are augite, subcalcic augite and rarer pigeonite. Hypersthene occurs in rare examples of the Kilauea basalts (average I.R. 0.59) whereas Macdonald (1949a) shows that in the Mauna Loa basalts (I.R. 0.64) microphenocrysts of hypersthene are present in a substantial minority of specimens and in the analysed Koolau basalts (I.R. 0.70) microphenocrysts of hypersthene are normal (Wentworth and Winchell, 1947).

Indicator ratio 0.50 to 0.39. The average Scottish plateau basalt (22, probably rather altered), olivine basalts from the Central Cascade Range (23) and the Tertiary tholeiites of south-western Australia (24) belong here. The suite appears to be transitional towards alkali olivine basalts. Edwards (1938) reports that augite and pigeonite are the pyroxenes of the Western Australian rocks, but in the suite as a whole hypersthene appears to be characteristically absent and pigeonite rare.

Indicator ratio 0.38 to 0.00. In the range 0.38 to 0.00 are Ascension Island (25), Banks Peninsula, New Zealand (26), Skjaldbreith shield volcano, Iceland (27), Tutuila (28), Easter Island (29), Galapagos (30), Medicine Lake Highlands of California (31), older series of Mauritius (32), Gambier Island (34), the Hamakua series of Mauna Kea (37), Juan Fernandez (38) and Réunion (33, 35, 36, 39). The alkali-silica ratio for Ascension basalts (mostly in fact hawaiites with normative ab>an) is essentially that characteristic of alkali olivine basalt suites (Tilley, 1950) and one new analysis shows a very small amount of normative nepheline. However, as in the case of the other provinces mentioned, most Ascension Island analyses show significant amounts of normative hypersthene and one analysed specimen to be described elsewhere contains modal hypersthene and a siliceous pegmatoid. Otherwise hypersthene appears to be virtually unknown in these suites and pigeonite is rare or absent. It is usual for olivine to occur as groundmass microlites as well as phenocrysts (*e.g.* Lacroix, 1936) without obvious reaction relationship to pyroxene and for augite or titanaugite to appear sometimes as phenocrysts as well as in the groundmass. A group of Réunion oceanites (38) illustrates the effects on the diagram of olivine accumulation.

The Skjaldbreith lavas (Tryggvason, 1943) are of tholeiitic aspect in their low alkali/silica ratio and the high-alumina basalts of the Medicine Lake Highlands (Anderson, 1941) while variable in alkali and normative hypersthene contents, tend also to have rather low alkali/silica ratios. Apart from these two magma-batches, the others cited may be described as mildly alkaline in the sense that even though the analyses show minor normative hypersthene, they have relatively high ratios of alkalis to silica. This results in the common presence of groundmass alkali feldspar. Such suites are in fact commonly referred to in petrological literature as olivine basalts of alkaline type. It is notable that those from Réunion, Easter Island, Galapagos, Banks Peninsula, Tutuila and Ascension all have pantellerites or pantelleritic trachytes as associates while the older volcanic series of Mauritius includes trachytes that may be either slightly oversaturated or moderately undersaturated

(Lacroix, 1936; Bandy, 1937; Richardson, 1933; Speight, 1938; Daly, 1924; 1925; Walker and Nicolaysen, 1954).

Nepheline present in norm. The average Japanese alkali basalt (40), Hualalai, Hawaii (41), St. Helena (42), Bora-Bora and neighbouring islands of the N.W. Society Islands (43), and younger basalts of Mauritius (44) are representatives of typical undersaturated alkali basalt suites. On St. Helena the differentiation trend is clearly phonolitic (Daly, 1927). Finally, averages are plotted for five more strongly alkaline, basanitic provinces having indicator ratios −0.30 to −0.40, namely Rungwe Volcano, East Africa (45), the peripheral subprovince of the Dunedin district (46), Auckland city (47), Tahiti (48) and basanites of the Honolulu series, Oahu (49). For all these more alkaline basalts the pyroxene is typically titanaugite, olivine occurs both as phenocrysts and in the groundmass and a reaction relationship between olivine and a lime-poor pyroxene is unknown, although reaction between olivine and titanaugite has been reported.

Discussion. The above survey suggests that, at least in a general way, there is a close correlation between the normative composition of magma batches, the pyroxene crystallization history and ultimate differentiation trends. Typical tholeiites showing a strong reaction relationship and yielding granophyric differentiates, more mildly tholeiitic types such as those of Kilauea, mildly alkaline and transitional types which follow a pantelleritic or trachytic trend, and finally the more strongly alkaline types differentiating to phonolite, appear to plot in an essentially continuous band across the diagram. There is a heavy clustering of points representing the most voluminous and typical tholeiites. Nevertheless, in terms of the variables here considered and in confirmation of the views of Green and Poldervaart (1955) and others, there appears to be a continuous series of basaltic magmas ranging from calcalkaline and tholeiitic at one extreme through transitional types to the typical alkali basalts and thence to the basanites.

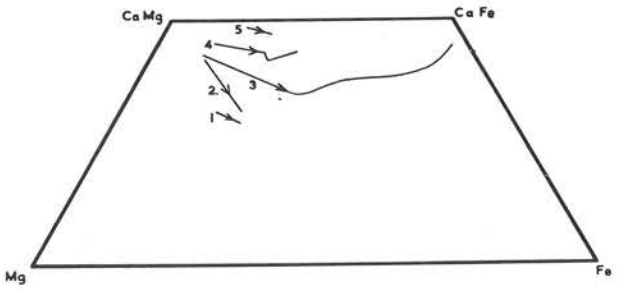

FIG. 5. Some clinopyroxene trends in terms of relative proportions of Ca, Mg, Fe.

1. Prehistoric flow, Kilauea (Yoder and Tilley, 1957).
2. Kilauea flow of 1921 (Yoder and Tilley, 1957).
3. Skaergaard (Brown, 1957; Muir, 1951).
4. Garbh Eilean (Murray, 1954).
5. Black Jack teschenite (Wilkinson, 1957).

Interrelation Between Pyroxene and Host Rock

The familiar Di-En-Fs-He or Ca-Mg-Fe diagram (Fig. 5) clearly portrays the progressive relative variation of Ca, Mg and Fe in pyroxenes during fractionation of basic magmas. It is generally believed that pyroxene crystallization history is of fundamental importance to the mutual relationship of tholeiitic and alkali basalt magmas, in effect to questions of saturation or undersaturation in silica. It would be helpful to have a projection of pyroxene compositions which had a direct bearing on this problem, and a norm, calculated from pyroxene analyses, appears to be a convenient starting point for this purpose. Many examples are set out in Tables 2–7.

The alumina of pyroxene analyses appears in the norm as feldspars or feldspathoids[1] and inspection will show that for the clinopyroxenes treated, normative feldspar ranges from 3.5 to 27.2% by weight. Furthermore almost all analyses examined contain significant amounts of normative olivine, and in the case of pyroxenes from alkaline rocks, normative nepheline and sometimes leucite and calcium orthosilicate as well. In the Pl-Di-Ol-Qz tetrahedron, clinopyroxene compositions thus plot somewhat above the base and occupy an irregular volume stretching from the Pl-Di-Hy plane to the Pl-Di-Ol face and thence into the neighbouring Pl-Ne-Di-Ol tetrahedron.

In the case of one analysis examined, Table 5, No. II, from the strongly alkaline Black Jack Sill, N.S.W. (Wilkinson, 1957), a total of 12.7% normative Ca_2SiO_4+Il+Mt cannot be represented within the tetrahedra employed. Usually however, not more than a few per cent of the pyroxene components are unaccounted for. It is of interest to note that clinopyroxene analyses commonly contain only 70–90% of normative pyroxene components, in one case examined (Table 4, No. 26) only 58%. In such rocks,

[1] Also as corundum in the case of the high-alumina enstatites of peridotitic inclusions in basaltic rocks.

substantially more pyroxene should appear in the mode than in the norm.

Skaergaard and Stillwater (*Fig. 6, Tables 2, 3*). The chemical analysis of augitic pyroxene from the Skaergaard border group gabbro-picrite (Brown, 1957) contains a negligible trace of normative nepheline. In Brown's series (1957, 1960) from augite to ferroaugite, not only do the augitic pyroxenes become more iron-rich and lime-poor (*cf.* Fig. 5), their analyses are also seen to move progressively in terms of normative components (Fig. 6) from the Di-Ol join to the metasilicate join, becoming effectively saturated in silica in the middle gabbros (nos. 5, 6). Brown (1957) and Muir (1951) have demonstrated that for still more iron-rich compositions, not normally attained in basaltic crystallization, the later clinopyroxenes become progressively more lime-rich again, a fact reflected by migration of the later members of the series back towards the $Ca(MgFe)Si_2O_6$ apex of Fig. 6. Skaergaard olivines (Wager and Deer, 1939, pp. 72–73), bronzite and pigeonites (Brown, 1957) are plotted on the same diagram. One of the olivine analyses contains normative Ca_2SiO_4 which is not represented on the diagram.

For comparative purposes, five clinopyroxenes and five orthopyroxenes from the Stillwater Complex (Hess, 1960) are also plotted. In Fe/(Fe+Mg) ratio these correspond to the two most iron-poor of the Skaergaard augites.

TABLE 2. SKAERGAARD PYROXENES

Norms (weight per cent)

Ref. No.	1	2	3	4	5	6	7	8	9	10	11	1′	4′	6′	7′
qz	—	—	—	—	—	0.2	—	—	—	—	—	—	—	—	—
or	0.3	0.3	0.2	0.4	0.1	0.1	0.2	0.2	0.1	0.1	0.2	0.2	—	0.2	0.6
ab	5.4	3.1	3.3	3.0	2.2	2.2	2.0	2.1	2.1	2.0	1.9	1.7	—	0.8	1.6
ne	0.1	—	—	—	—	—	—	—	—	—	—	—	—	—	—
an	5.7	6.3	4.7	4.9	5.0	4.2	4.8	4.6	2.4	2.6	1.8	5.3	6.2	4.4	2.5
di {di	68.2	53.6	48.7	47.4	41.2	39.0	36.1	35.1	34.2	31.8	13.9	3.0	8.0	6.9	7.1
di {he	7.6	17.3	20.2	21.1	24.6	26.4	26.8	28.6	32.4	39.8	66.1	0.7	5.3	6.7	7.7
hy {en	—	8.6	10.4	9.8	13.9	13.9	13.6	12.9	11.6	7.6	1.9	64.7	40.1	37.1	33.4
hy {fs	—	3.2	5.0	5.0	9.5	10.8	11.6	12.0	12.5	11.0	10.3	16.5	30.2	41.1	42.2
ol {fo	7.0	2.8	1.9	2.6	0.3	—	0.7	0.4	0.3	0.7	0.2	3.8	4.3	0.4	1.4
ol {fa	1.0	1.1	1.0	1.5	0.2	—	0.7	0.4	0.3	1.2	1.0	1.1	3.6	0.4	1.8
il	1.8	1.4	1.8	2.5	1.5	1.6	1.2	1.4	2.5	1.5	1.3	0.9	1.0	0.9	0.8
mt	2.2	2.5	2.7	1.9	1.8	1.8	2.3	2.5	2.2	2.2	2.1	1.9	1.6	1.0	0.9
cm	0.6	0.2	0.1	—	—	—	—	—	—	—	—	0.4	—	—	—
Total	99.9	100.4	100.0	100.1	100.3	100.2	100.0	100.2	100.6	100.5	100.7	100.2	100.3	99.9	100.0
Molecular proportions $NaAlSiO_4$: $Ca(Mg, Fe)Si_2O_6$: $(Mg, Fe)SiO_3$: $(Mg, Fe)_2SiO_4$: SiO_2															
$NaAlSiO_4$	0.1	—	—	—	—	—	—	—	—	—	—	—	—	—	—
$Ca(Mg, Fe)Si_2O_6$	86.3	70.2	65.7	65.3	57.7	56.1	54.2	55.3	57.4	64.3	76.2	2.0	7.9	7.9	8.7
$(Mg, Fe)SiO_3$	—	24.3	30.3	29.2	41.8	43.2	44.2	43.8	41.9	33.4	22.4	94.1	85.5	91.5	88.7
$(Mg, Fe)_2SiO_4$	13.6	5.5	5.0	5.5	0.5	—	1.6	0.9	0.7	2.3	1.4	3.9	6.6	0.6	2.6
SiO_2	—	—	—	—	—	0.7	—	—	—	—	—	—	—	—	—
Atomic ratio Fe/Fe+Mg															
Fe/Fe+Mg	0.17	0.28	0.33	0.33	0.38	0.41	0.43	0.46	0.49	0.55	0.81	0.19	0.38	0.47	0.50

KEY TO TABLE 2 Norms of Skaergaard Pyroxenes

1. Augite from gabbro picrite, 4526 (Brown, 1957)
2. Augite from lower olivine gabbro, 30 m., 4392 (Brown, 1957)
3. Augite from lower olivine gabbro, EG4389 (Brown, 1960, p. 18)
4. Augite from lower olivine gabbro, 600 m., 4385A (Brown, 1957)
5. Augite from middle gabbro, 1060 m., 4369 (Brown, 1957)
6. Augite from middle gabbro, 1310 m., 4341 (Brown, 1957)
7. Augite from ferrogabbro, 1600 m., 4430 (Brown, 1957)
8. Augite from ferrogabbro, 1740 m., 4306 (Brown, 1957)
9. Augite from ferrogabbro, 1830 m., 4309 (Brown, 1957)
10. Ferroaugite from ferrogabbro, 2000 m., 4314 (Brown, 1957)
11. Ferroaugite from ferrogabbro, EG 4318 (Brown, 1960, p. 18)
1′. Bronzite from gabbropicrite, 4526 (Brown, 1957)
4′. Pigeonite from lower olivine gabbro 4385A (Brown, 1957)
6′. Pigeonite from middle gabbro 4341 (Brown, 1957)
7′. Pigeonite from ferrogabbro 4430 (Brown, 1957)

Contrasting pyroxenes from alkaline and tholeiitic provinces. Norms of phenocrystic and groundmass pyroxenes from hawaiites, mugearites and Japanese alkali dolerites are set out in Table 4. Those of pyroxenes from the Black Jack teschenite sill (Wilkinson, 1957, 1958) and the Garbh Eilean picritic and crinanite sill (Murray, 1954), are set out in Table 5. Norms of pyroxenes from tholeiitic rocks are recorded in Tables 2, 3 and 6. The pyroxenes listed in Tables 4, 5 and 6 are plotted in Fig. 7 and fields for pyroxenes of all tables are summarized on the same diagram. Clearly, clinopyroxenes from alkaline basaltic rocks (field A) differ from those of tholeiites (field B) not only in a tendency towards a higher Ca/(Mg+Fe) ratio (*cf.* Fig. 5) and higher titanium content, but also in a greater degree of silica undersaturation in terms of normative components. Thus normative nepheline is absent from only 3 of 23 pyroxene analyses examined from alkaline basaltic rocks, and the exceptions (42–44, Table 5) are all from the upper portions of the mildly alkaline Garbh Eilean Sill. In contrast tholeiitic pyroxenes from Japan (Kuno, 1955) and Hawaii range from diopside-rich compositions near the Di-Ol join to subcalcic

TABLE 3. PYROXENES FROM THE STILLWATER COMPLEX, MONTANA

Norms (weight per cent)

Ref. no.	11A	12	13	14	15	16	17	18	19	20	21
Authors' No.	MVL 101/2	I52	EB175	EB43	EB41	7666	7704	EB13	EB38	EB130	EB41$_1$
qz	—	—	—	—	0.4	—	—	0.2	0.6	0.5	1.8
or	—	—	0.1	0.1	—	—	—	—	—	—	—
ab	2.4	2.7	2.4	2.3	1.9	—	—	—	—	—	0.4
ne	—	—	—	—	—	—	—	—	—	—	—
an	6.9	6.7	6.1	7.1	5.3	4.4	4.2	4.7	4.1	4.5	4.3
di (di)	58.6	63.6	63.2	56.2	51.9	2.1	1.7	2.3	3.5	2.6	11.0
di (he)	5.8	6.3	12.8	14.3	19.5	0.3	0.3	0.5	0.9	1.0	6.3
hy (en)	14.1	13.2	9.4	10.9	12.0	79.0	77.3	73.2	68.6	62.0	44.2
hy (fs)	1.6	1.5	2.2	3.2	5.2	12.1	14.9	17.3	20.7	26.8	29.1
ol (fo)	5.0	1.9	0.7	2.0	—	—	0.1	—	—	—	—
ol (fa)	0.6	0.2	0.2	0.7	—	—	0.0	—	—	—	—
il	0.5	0.5	0.8	0.9	1.0	0.2	0.2	0.3	0.4	0.5	0.7
mt	2.0	1.7	2.0	2.0	2.3	1.4	0.7	0.8	1.2	1.6	1.6
cm	1.6	1.7	—	—	—	0.7	0.8	0.7	0.1	0.1	—
Total	99.1	100.0	99.9	99.7	99.5	100.2	100.2	100.0	100.1	99.6	99.4
Molecular proportions $NaAlSiO_4$:$Ca(Mg, Fe)Si_2O_6$:$(Mg, Fe)SiO_3$:$(Mg, Fe)_2SiO_4$:SiO_2 recalculated to 100%											
$NaAlSiO_4$	—	—	—	—	—	—	—	—	—	—	—
$Ca(Mg, Fe)Si_2O_6$	60.6	66.9	74.6	67.8	65.6	1.2	1.0	1.4	2.3	1.9	9.9
$(Mg, Fe)SiO_3$	31.4	30.2	24.1	28.5	33.0	98.8	98.9	98.2	96.5	97.1	86.2
$(Mg, Fe)_2SiO_4$	8.0	2.9	1.3	3.7	—	—	0.1	—	—	—	—
SiO_2	—	—	—	—	1.4	—	—	0.4	1.2	1.0	3.9
Atomic ratio Fe/Fe+Mg											
Fe/Fe+Mg	0.14	0.13	0.20	0.23	0.30	0.12	0.14	0.16	0.20	0.27	0.35

$_1$ Augite impurity.

KEY TO TABLE 3

Norms of Stillwater pyroxenes
Specimen numbers as in Hess (1960, pp. 25, 28, 36)

11A–15. Clinopyroxenes.
16–20. Orthopyroxenes of Bushveld Type.
21. Orthopyroxene of Stillwater Type (inverted pigeonite).

augites or pigeonitic augites which lie near the metasilicate join. Two analyses of iron-poor phenocrystic augites from Taga Volcano, Japan (Kuno, 1955) show trace amounts of normative nepheline and can in this respect be compared with the earliest Skaergaard augite, but the other analyses examined show normative hypersthene and olivine or occasionally minor quartz.

Lines are drawn connecting a number of the pyroxenes to points representing their host rocks. It is to be emphasized that the host rock compositions shown will not in general represent the composition of the melt phase at the time the pyroxene was crystallizing. Nevertheless the orientations of these tie-lines suggest that the degree of effective undersaturation of the pyroxene bears a crude relationship to the degree

TABLE 4. PYROXENES FROM ALKALINE BASALTIC ROCKS

Norms (weight per cent)

Ref. No.	22	23	24	25	26	27	28	29	30	31
qz	—	—	—	—	—	—	—	—	—	—
or	0.6	0.4	1.7	0.3	4.0	0.3	3.5	0.5	1.3	—
lc	—	—	—	—	—	—	—	—	—	1.3
ab	3.0	3.4	6.7	0.3	11.0	3.6	11.8	6.8	0.2	—
ne	1.0	5.2	2.5	4.8	4.8	2.4	2.8	4.6	2.2	2.0
an	9.7	2.7	11.8	5.4	12.2	2.6	7.4	2.2	6.1	14.3
di di	61.1	68.6	54.9	64.8	46.7	59.7	43.0	29.3	67.4	51.9
di he	12.8	14.4	13.0	16.7	11.4	24.2	24.6	45.2	13.4	16.0
hy en	—	—	—	—	—	—	—	—	—	—
hy fs	—	—	—	—	—	—	—	—	—	—
ol fo	4.9	0.4	2.8	2.1	1.4	1.6	2.7	—	1.2	4.2
ol fa	1.3	0.2	0.8	0.7	0.4	0.8	1.9	—	0.3	1.6
cs	—	—	—	—	—	—	—	2.8	—	0.6
il	2.7	2.1	4.4	3.0	5.3	2.0	1.5	4.5	5.4	5.6
mt	2.8	3.2	1.8	3.4	2.7	3.3	0.9	4.6	3.1	2.1
cm	—	—	—	—	—	—	—	—	—	—
Total	99.9	100.6	100.4	101.5	99.9	100.5	100.1	100.5	100.6	99.6

Molecular proportions

$NaAlSiO_4$ $+KAlSi_2O_6$	1.7	8.9	5.1	8.0	10.9	4.2	5.6	9.3	3.9	5.5
$Ca(Mg, Fe)Si_2O_6$	78.8	90.3	88.1	87.7	85.1	92.1	86.1	90.7	93.5	84.0
$(Mg, Fe)SiO_3$	—	—	—	—	—	—	—	—	—	—
$(Mg, Fe)_2SiO_4$	19.5	0.8	6.8	4.3	4.0	3.7	8.3	—	2.6	10.5
SiO_2	—	—	—	—	—	—	—	—	—	—

Atomic ratio Fe/Fe+Mg

Fe/Fe+Mg	0.25	0.26	0.27	0.29	0.33	0.34	0.36	0.66	0.29	0.32

KEY TO TABLE 4

Pyroxenes from alkaline basaltic rocks

22. From hawaiite 60464, Papalele Gulch, Mauna Kea (Muir and Tilley, 1961, Table 9, No. 6).
23. From "soda mugearite" 72881, Ulva Ferry, Mull (Muir and Tilley, 1961, Table 9, No. 8).
24. From hawaiite 68219, Kahului, Maui (Muir and Tilley, 1961, Table 9, No. 3).
25. From mugearite basalt 7568, River Rha, above Uig, Skye (Muir and Tilley, 1961, Table 9, No. 2).
26. From hawaiite 57361, Noonaohae Cone, Mauna Kea (Muir and Tilley, 1961, Table 9, No. 4).
27. From "mugearite" (hawaiite) 76503, Jeffreys Hill, E. Otago, N. Z. (Muir and Tilley, 1961, Table 9, No. 12).
28. From mugearite, 9384, Druim na Criche, near Mugeary, Syke (Muir and Tilley, 1961, Table 9, No. 1).
29. From "mugearite" (hawaiite) 76505, Scroggs Hill, E. Otago, N. Z. (Muir and Tilley, 1961, Table 9, No. 13.)
30. Titanaugite from dolerite 1507, Tahara Bridge, Sakhalin (Yagi, 1953).
31. Titanaugite from dolerite 607, Morotu Cape, Sakhalin (Yagi, 1953).

of undersaturation of the host rock. From the figure it would seem that the effect of separation of clinopyroxene from those basaltic magmas that initially carry substantial amounts of normative Ne, will be to displace the liquid towards more strongly undersaturated compositions whereas magmas plotting clearly to the right of the Di-Ol join, will be displaced towards more siliceous compositions. Present data do not allow a decisive appraisal of the effect on silica saturation of the separation of pyroxenes, olivine or plagioclase from basaltic liquids lying close to the Di-Ol join, and hence to the plagioclase-diopside-olivine plane. Nevertheless a number of rock-pyroxene tie-lines plotted in this region are roughly parallel to the join and suggest that separation of pyroxene, like separation of olivine and plagioclase, may have little effect on the degree of silica saturation of such liquids. This accords with the observation already made that basaltic magma batches that appear to have differentiated towards trachyte, do in fact plot close to the Di-Ol join.

Chromian diopsides from peridotitic inclusions in basaltic rocks. Norms (Table 7) have been calculated for the ten modern analyses of chromian diopsides listed by Ross *et al.* (1954), eight of them from the peridotitic inclusions commonly found in alkaline basaltic rocks, and two from dunites. In spite of the presence of appreciable Cr_2O_3 and TiO_2 which in the norm calculation are combined with FeO releasing SiO_2 for other purposes, all but two of the analyses of diopsides from inclusions carry normative nepheline. The analyses of these plot in a field C (Fig. 7), overlapping that of pyroxenes from alkaline basaltic rocks, but with its centre of gravity nearer the Di-Ol join and displaced somewhat towards the olivine point.

Hawaiian tholeiitic basalts and their pyroxenes. Variants of the Kilauea flows of 1921 (*e.g.* Tilley, 1960a), 1959 (Tilley, 1960b), 1955 (Macdonald, 1955), 1840 (Macdonald, 1949b), the Uwekahuna laccolith of Kilauea (Murata and Richter, 1961), the Mauna Loa and Kilauea flows of 1868 (Tilley and Scoon, 1961) and Palolo quarry, Oahu (Kuno *et al.*, 1957) are plotted on Fig. 8 together with the 1887 hypersthene basalt of Mauna Loa (illey, 1961) and average Koolau basalt. In each case the points for each suite fall in a well defined band, in general order of increasing ratio of Fe/Mg from left to right, the sharpness of the

TABLE 5. PYROXENES FROM THE BLACK JACK (32–35) AND GARBH EILEAN (36–44) SILLS

(Data from Wilkinson, 1957 and Murray, 1954)

Norms (weight per cent)

Ref. No.	32	33	34	35	36	37	38	39	40	41	42	43	44
Author's No.	I	II	III	IV	I	17	20	P1	31L	P2	25	29	31H
or	—	—	—	0.2	—	—	tr.	tr.	tr.	tr.	tr.	0.3	tr.
lc	0.2	0.5	0.6	0.2	tr.	tr.	—	—	—	—	—	—	—
ab	—	—	—	—	—	—	1.8	0.7	2.2	1.9	3.7	1.0	2.6
ne	3.0	3.7	3.2	3.1	1.8	2.1	1.0	2.8	0.2	2.4	—	—	—
an	15.0	11.7	6.3	8.0	7.3	6.2	8.3	7.6	9.3	7.0	5.7	8.4	5.8
di {di	56.9	57.2	57.7	55.6	68.4	70.0	67.2	64.6	63.6	68.1	56.7	50.2	44.6
di {he	9.9	11.0	21.3	25.0	8.8	8.6	11.8	14.2	14.1	11.8	23.4	22.7	34.4
hy {en	—	—	—	—	—	—	—	—	—	—	1.2	5.8	2.4
hy {fs	—	—	—	—	—	—	—	—	—	—	0.6	3.0	2.1
ol {fo	3.0	2.7	1.4	0.9	4.0	4.5	3.2	3.3	3.4	1.2	2.5	1.8	1.7
ol {fa	0.7	0.6	0.7	0.5	0.7	0.7	0.7	0.9	1.0	0.3	1.3	1.0	1.7
cs	3.6	3.9	1.6	—	3.3	1.6	—	—	—	—	—	—	—
il	5.8	6.1	4.6	4.1	3.5	2.7	2.6	4.3	2.4	4.1	2.5	2.6	2.6
mt	2.2	2.7	2.6	2.1	2.7	3.9	3.7	1.7	3.3	3.4	2.5	3.4	2.2
Total	100.3	100.1	100.0	99.7	100.5	100.3	100.3	100.1	99.5	100.2	100.1	100.2	100.1
Molecular proportions $NaAlSiO_4$+$KAlSi_3O_8$:$Ca(Mg, Fe)Si_2O_6$:$(Mg, Fe)SiO_3$:$(Mg, Fe)_2SiO_4$													
$NaAlSiO_4$+$KAlSi_3O_8$	6.2	7.9	6.4	5.8	3.3	3.6	1.7	4.9	0.4	4.3	—	—	—
$Ca(Mg, Fe)Si_2O_6$	86.8	85.9	90.1	91.8	88.8	87.8	91.5	88.2	92.0	93.1	84.6	76.8	85.0
$(Mg, Fe)SiO_3$	—	—	—	—	—	—	—	—	—	—	3.8	19.0	9.9
$(Mg, Fe)_2SiO_4$	7.0	6.2	3.5	2.4	8.0	8.7	6.8	6.9	7.6	2.6	11.6	4.2	5.1
Atomic ratio Fe/Mg+Fe													
Fe/Fe+Mg	0.27	0.29	0.35	0.37	0.21	0.22	0.25	0.25	0.27	0.27	0.34	0.36	0.46

bands having been somewhat improved by reducing Fe_2O_3 to an arbitrary value based on the least oxidized specimens and increasing FeO accordingly. The value of 1.5% has been used except for Kilauea 1955 for which 1.87% Fe_2O_3 has been used. In the case of the rather highly oxidized Palolo quarry variants two points are shown for each analysis, that on the right representing the unadjusted analysis, the other after reduction of Fe_2O_3 to 1.5%.

Also shown are points for the five pyroxene analyses so far available: two fractions of augitic pyroxene separated from the 1840 picrite basalt, clinopyroxene and hypersthene from the Uwekahuna laccolith, and pigeonitic groundmass augite from the

TABLE 6. PYROXENES FROM SOME THOLEIITIC AND RELATED ROCKS OF JAPAN AND HAWAII

Norms (weight per cent)

Ref. No.	45	46	47	48	49	50	51	52	53	54	55	56	57
qz	—	—	—	—	—	—	—	—	—	—	1.5	1.1	—
or	0.0	—	1.0	0.7	0.7	0.4	0.9	0.8	0.1	0.3	1.2	1.5	0.2
ab	0.0	—	2.7	0.7	2.9	2.7	3.2	2.8	2.7	3.8	5.9	8.1	1.4
ne	—	0.9	—	0.7	—	—	—	—	—	—	—	—	—
an	14.9	12.5	3.8	6.0	4.5	—	—	0.8	7.1	8.3	7.2	9.4	5.0
ac	—	—	—	—	—	0.8	2.0	—	—	—	—	—	—
di di	67.1	60.3	61.9	73.4	25.1	23.5	24.0	25.8	61.0	58.7	42.7	25.3	5.3
di he	8.4	13.5	13.9	10.7	12.4	15.3	16.3	28.8	9.8	10.0	11.7	10.5	1.5
hy en	—	—	5.0	—	19.2	26.9	22.6	14.9	8.5	8.5	18.1	27.2	60.0
hy fs	—	—	1.3	—	10.8	20.2	17.5	19.1	1.6	1.6	5.8	12.9	18.8
ol fo	4.4	6.3	5.1	3.1	12.8	2.2	4.6	2.5	4.6	4.3	—	—	2.8
ol fa	0.7	1.8	1.5	0.6	8.0	1.8	4.0	3.5	0.9	0.9	—	—	1.0
cs	0.1	2.3	—	—	—	—	—	—	—	—	—	—	—
il	0.8	0.8	1.4	0.5	0.6	1.4	1.1	0.3	1.4	1.7	2.7	1.8	2.1
mt	3.5	1.1	1.5	4.0	2.9	5.0	3.8	0.5	1.8	1.3	2.4	1.6	1.6
cm	—	—	—	—	—	—	—	—	0.7	0.8	0.8	—	0.2
Total	99.9	99.5	99.1	100.4	99.9	100.2	100.0	99.8	100.2	100.2	100.0	99.4	99.9
Molecular proportions $NaAlSiO_4$:$Ca(Mg, Fe)Si_2O_6$:$(Mg, Fe)SiO_3$:$(Mg, Fe)_2SiO_4$:SiO_2													
$NaAlSiO_4$	—	1.6	—	1.3	—	—	—	—	—	—	—	—	—
$Ca(Mg, Fe)Si_2O_6$	90.8	84.7	76.8	92.7	29.1	27.4	30.1	41.7	70.6	70.3	49.5	29.1	3.8
$(Mg, Fe)SiO_3$	—	—	13.4	—	48.0	68.7	61.0	52.1	21.3	21.8	45.4	67.5	93.1
$(Mg, Fe)_2SiO_4$	9.2	13.6	9.8	6.0	22.9	3.9	8.9	6.2	8.1	7.9	—	—	3.1
SiO_2	—	—	—	—	—	—	—	—	—	—	5.1	3.3	—
Atomic ratio Fe/Fe+Mg													
Fe/Fe+Mg	0.19	0.20	0.21	0.21	0.34	0.42	0.42	0.50	0.18	0.18	0.27	0.30	0.22

KEY TO TABLE 6

Pyroxenes from some tholeiitic and related rocks of Japan and Hawaii

A. *Salite and augite phenocrysts, Hakone and Taga Volcanoes, Japan*

45. Salite phenocrysts, basalt tuff, Taga Volcano (Kuno, 1955, No. 2, p. 73).
46. Salite phenocrysts, olivine eucrite in tuff, Taga Volcano (Kuno, 1955, No. 1, p. 73).
47. Augite phenocrysts, hypersthene-olivine-augite andesite, Hakone (Kuno, 1955, No. 5, p. 74).
48. Augite phenocrysts, olivine-augite basalt, Taga Volcano (Kuno, 1955, No. 4, p. 73).

B. *Groundmass subcalcic augites from Japanese tholeiites*

49. From aphyric basalt, Okata, Ō-Sima (Kuno, 1960, No. 3, p. 128).
50. From pyroxene basalt flow of 1778, Ō-Sima (Kuno, 1955, No. 9, p. 75).
51. From hypersthene-augite basalt, extruded 1950, Ō-Sima Island (Kuno, 1955, No. 8, p. 75).
52. From olivine basalt, Hatu-Sima, east of Taga (Kuno, 1955, No. 7, p. 74).

C. *Clinopyroxenes from Hawaii*

53. From Uwekahuna gabbroic laccolith, Kilauea (Muir and Tilley, 1957, Table 4).
54. Phenocrysts from picrite basalt flow of 1840, Nanawale Bay (Muir and Tilley, 1957, Table 4).
55. Groundmass clinopyroxene, picrite basalt flow of 1840, as for No. 54.
56. Pigeonitic augite of groundmass, hypersthene-olivine basalt of 1887, Mauna Loa (Tilley, 1961).

D. *Hypersthene from Hawaii*

57. From Uwekahuna laccolith, as for No. 53.

hypersthene basalt of 1887. In addition the Ca-Mg-Fe ratios of successive clinopyroxene fractions from the 1921 Kilauea flows are known (Muir *et al.* 1957) and their general position within the field of tholeiitic pyroxenes can be confidently predicted.

At least two trends are clearly shown by the rock suites. The first of these is approximately away from the olivine point and graphically demonstrates the effect of olivine separation and accumulation. Thus Uwekahuna no. 1 represents the lower chilled margin of the intrusion and 6 the upper margin, whereas 2, 3 and 4 represent olivine-enriched phases. In the case of the 1840 variants, if indeed they have a common parent, some separation of pyroxene as well as olivine is indicated as already concluded by Muir *et al.* (1957), the necessary crystal extract having a pro-

TABLE 7. CHROMIAN DIOPSIDES FROM PERIDOTITIC INCLUSIONS IN BASALTIC ROCKS (58–65) AND FROM TWO DUNITES (66–67)

Norms (weight per cent)

Ref. No.	58	59	60	61	62	63	64	65	66	67
Authors' No.	8	7	1	3	2	4	9	11	12	13
qz	—	—	—	—	—	—	—	—	—	—
or	0.4	0.2	0.5	0.4	0.6	0.5	0.1	0.2	0.2	0.6
ab	8.6	2.7	7.7	6.9	5.7	8.6	2.8	4.9	3.3	3.2
ne	5.2	1.9	0.7	2.7	3.2	0.9	—	—	—	—
an	1.3	9.5	9.0	11.4	9.9	12.0	3.2	9.7	—	—
ac	—	—	—	—	—	—	—	—	0.5	—
di (di)	72.3	72.0	69.7	61.7	66.0	57.9	73.9	65.5	82.4	82.5
di (he)	1.6	4.7	2.0	2.2	3.9	3.9	5.0	4.6	4.6	6.2
hy (en)	—	—	—	—	—	—	5.5	1.7	0.3	—
hy (fs)	—	—	—	—	—	—	0.4	0.1	0.0	—
ol (fo)	5.3	5.1	5.3	8.9	6.8	12.1	3.5	6.4	5.9	4.3
ol (fa)	0.1	0.4	0.2	0.4	0.5	1.0	0.3	0.6	0.5	0.4
cs	—	—	—	—	—	—	—	—	—	1.2
il	1.5	0.6	0.7	1.5	0.5	0.5	1.2	1.4	0.3	0.2
mt	1.2	1.0	2.5	2.2	2.1	1.2	2.3	3.7	0.2	—
cm	2.1	1.5	1.4	1.4	1.2	1.8	1.6	1.8	1.3	1.0
Total	99.6	99.6	99.7	99.7	100.4	100.4	99.8	100.6	100.2[1]	99.9[2]
Molecular proportions $NaAlSiO_4$+$KAlSi_2O_6$:$Ca(Mg, Fe)Si_2O_6$:$(Mg, Fe)SiO_3$:$(Mg, Fe)_2SiO_4$:SiO_2										
$NaAlSiO_4$	8.8	3.2	1.2	5.0	5.6	1.6	—	—	—	—
$Ca(Mg, Fe)Si_2O_6$	82.0	87.3	88.5	77.7	81.4	74.5	81.1	82.9	89.4	92.5
$(Mg, Fe)SiO_3$	—	—	—	—	—	—	13.1	4.7	0.7	—
$(Mg, Fe)_2SiO_4$	9.3	9.5	10.3	17.3	13.0	23.9	5.8	12.4	9.9	7.5
SiO_2	—	—	—	—	—	—	—	—	—	—
Atomic ratio Fe/Fe+Mg										
Fe/Fe+Mg	0.09	0.11	0.11	0.12	0.12	0.13	0.14	0.14	0.06	0.07

[1] Includes ns 0.7.
[2] Includes ns 0.3.

KEY TO TABLE 7

(Data from Ross *et al.*, 1954, p. 709)

A. *Chromian diopsides from peridotitic inclusions in basaltic rocks*

58. Salt Lake Crater, Honolulu Series, Oahu, Hawaii.
59. Ichinomegata, Japan.
60. Chihuahua, Mexico.
61. Peridot Cove, Arizona.
62. Ludlow, California.
63. Dreiser Weiher, Eifel, Germany.
64. Grove Farm Quarry, Kauai, Hawaii.
65. Flow of 1801, Hualalai, Hawaii.

B. *Diopsides from "dunites"*

66. Twin Sisters, Whatcom County, Washington.
67. Webster, North Carolina.

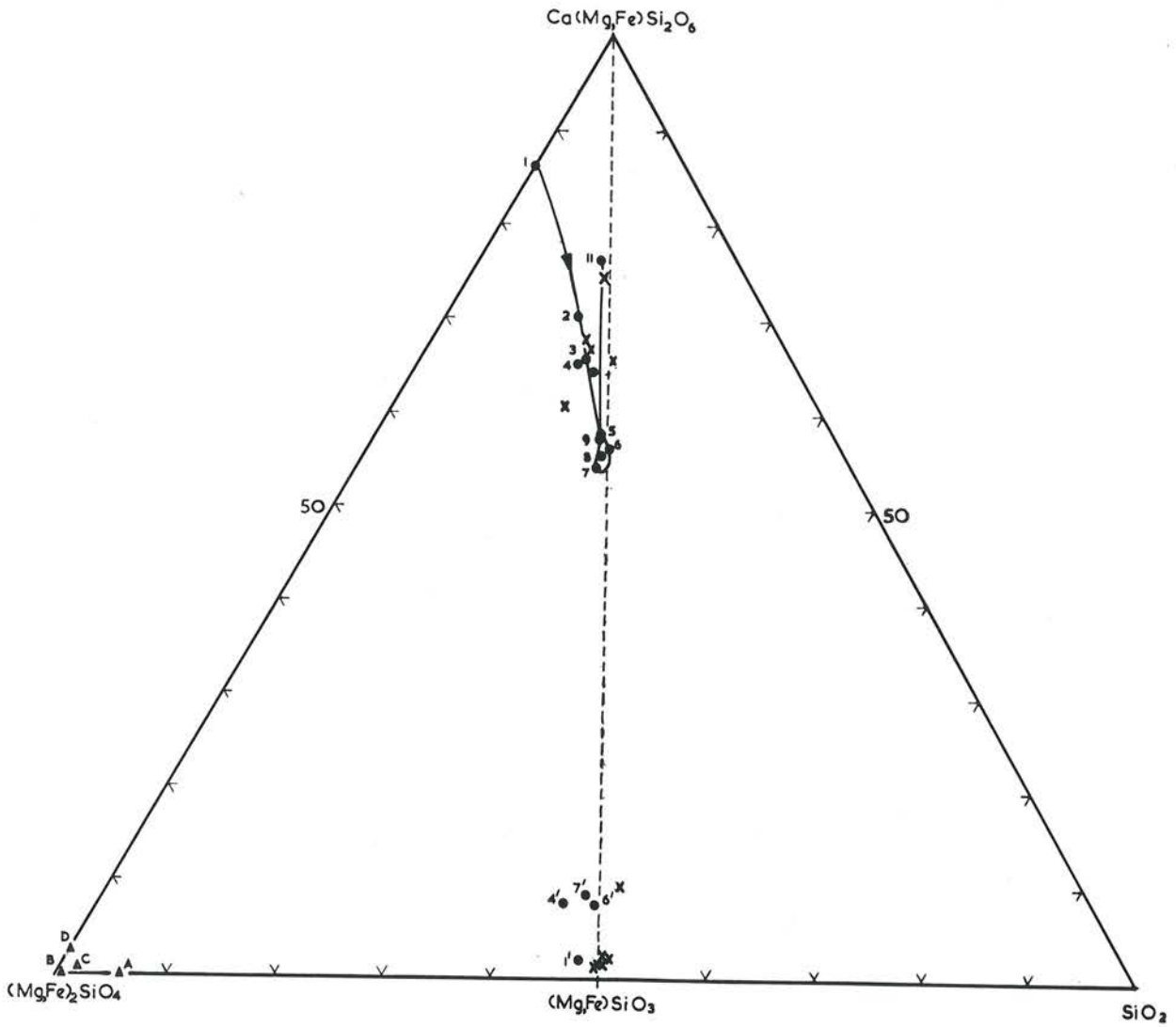

FIG. 6. Normative compositions of pyroxenes and olivines from the Skaergaard and Stillwater complexes in molecular proportions ferroan diopside:olivine:silica.

● Skaergaard pyroxenes 1 to 11; 1′–7′ (see Table 2).

× Stillwater pyroxenes (see Table 3).

▲ Skaergaard olivines A–D (olivines I to IV of Wager and Deer, 1939, pp. 72, 73).

jected composition such as E given by the intersection of the lava trend line with a join from the olivine point to the appropriate clinopyroxene composition. The same may apply to the 1921 variants. The trachyte and Pele's hair which constitute the least basic variants, numbers 5 and 6, of the 1921 suite, may well have reached the limits of the olivine field, and the same applies to the 1955 Kilauea lavas. These follow a trend athwart the trend of olivine separation, a trend clearly controlled by the separation of clinopyroxene. The more basic members of the 1955 series may well approximate to the position of an olivine-augitic pyroxene-plagioclase-liquid four-phase curve. Hypersthene appears in the less basic members, that is those having indicator ratio greater than about 0.60.

Late segregation veins (no. 7) from the Uwekahuna laccolith continue the 1955 trend and in a general way the Palolo quarry quartz dolerite and granophyres extend it still further. These rocks appear to represent liquids which have left the olivine surface entirely (a few deeply corroded relics remain) and are moving along a two pyroxene-feldspar-liquid four-phase curve, one of the pyroxenes ultimately no

doubt disappearing. In the Uwekahuna rocks and in the 1840 picrite basalt (indicator ratio approximately 0.55) the early pyroxene appears to be augitic pyroxene. On the other hand in the Koolau basalts (I.R.=0.70) and apparently in the 1868 and 1887 Mauna Loa flows (I.R. 0.62–0.65) hypersthene appears early, to be joined by pigeonitic augite. Separation of olivine in these cases presumably displaces the liquid to an olivine-*hypersthene*-plagioclase-liquid four-phase curve which must then be followed to the five-phase "point." A trend in this direction is suggested by the Izu basalt whole-rock and groundmass fractions (Fig. 4, Nos. 2 and 4). It is to be emphasized again that in the natural rock systems the four-phase curves and five-phase "point" are not fixed in position but will migrate with changing ratios of Fe/Mg, albite/anorthite and other variables; the present approach merely fixes their approximate position for typical magma compositions.

A Model for Tholeiitic Crystallization

The inferred relationships are summarized in Fig. 9 which is to be compared with Fig. 3. Figure 9 is a reconstruction of the inferred form of the plagioclase surface projected onto the base of the tetrahedron plagioclase-ferroan diopside-olivine-silica for natural basaltic compositions. A five-phase reaction point R is indicated in the general region $Di_{26}Hy_{54}Qz_{20}$ in normative molecular proportions. The width of the immiscibility gap shown between the two pyroxene composition fields is undoubtedly variable, being a

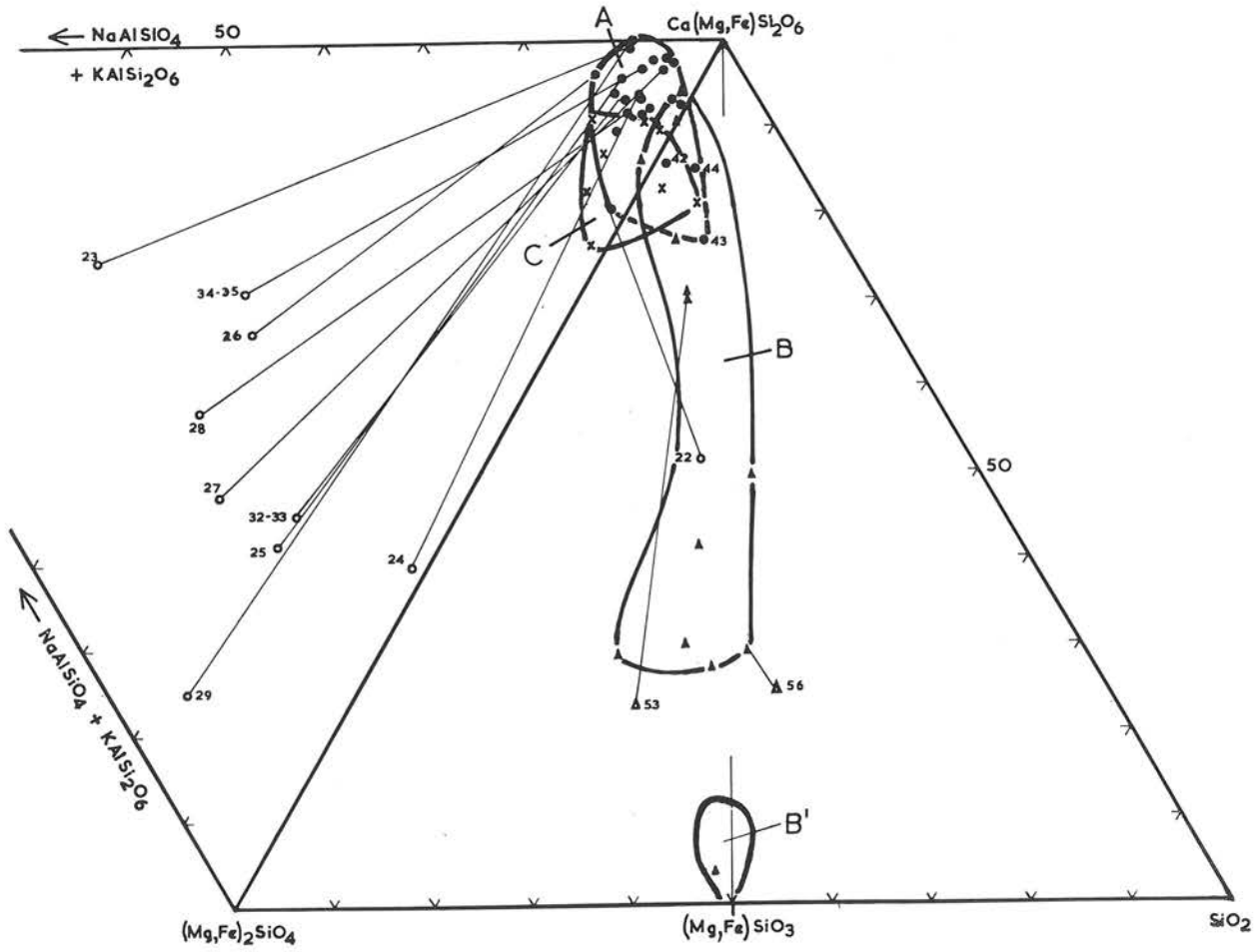

Fig. 7. Pyroxenes from alkaline basaltic rocks (field A), tholeiites (field B) and peridotitic inclusions (field C) and bulk composition of some host rocks. Compositions in molecular percentages of normative components. For explanation of numbers, see Tables 4–7.

●——○ Pyroxenes of alkaline basaltic rocks (solid symbols) and host rock (open symbols).

▲——△ Pyroxenes of tholeiitic rocks (solid symbols) and their host rock (open symbols).

× Pyroxenes from peridotitic inclusions in basaltic rocks.

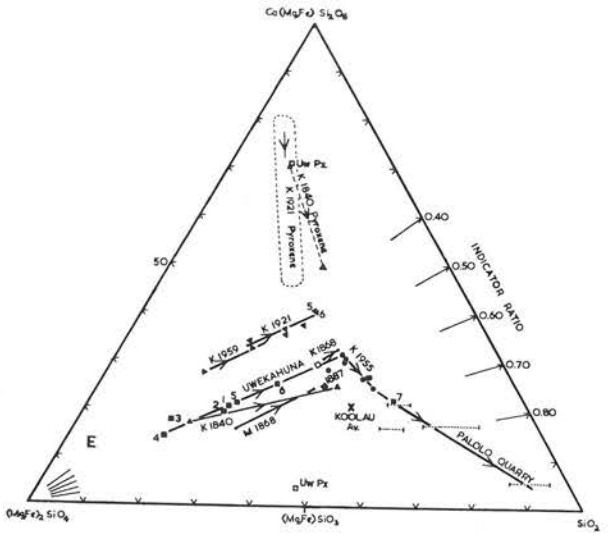

FIG. 8. Some Hawaiian differentiation trends. Solid symbols: rock analyses; open symbols: pyroxenes.

K1921: Kilauea 1921 lava variants; similarly for K1840, etc.

M1868: Mauna Loa 1868 lava variants.

Arrows indicate direction of increasing ratio Fe:Mg. For discussion, see text.

function of magmatic temperatures and pressures as well as Fe/Mg ratios. It is normally wider in intrusive rocks than it is in extrusives.

It is commonly considered that crystallization of hypersthene will give way to pigeonite when the pyroxene inversion temperature falls below the magma temperature. It should also be borne in mind (Gunn, 1962) that as the molar volume of pigeonite appears to be higher than that of a corresponding hypersthene-augite assemblage, intratelluric high-pressure crystallization will tend to extend the field of hypersthene with respect to that of pigeonite. Although the procedure of the present paper allows the approximate position of the five-phase point to be determined for a series of magmas, it does not portray the contrasting conditions for early separation of pigeonite as against hypersthene.

As demonstrated by Yoder and Tilley (1957), typical Hawaiian lavas commence to precipitate olivine, plagioclase and pyroxene within a relatively narrow temperature range. A liquid such as X is comparable to the 1921 and 1959 Kilauea magmas. Early separation of olivine should lead to a projected line of descent to point L on the olivine-augite-liquid surface on or near the plagioclase-olivine-augite-liquid curve. At this stage augite such as L′ should begin to crystallize, the liquid then following the course LMR, and the coexisting pyroxene the course L′M′R′. Hence if equilibrium were preserved, the residual liquid from liquid X would reach some point between M and R where the last trace of liquid would be in equilibrium with a homogeneous subcalcic augite of composition lying on the straight line X-L. If the relations are correctly drawn, olivine will continue to crystallize in minor amount together with pyroxene for liquids on the field boundary near L, but for liquids somewhere between M and R, the projected tie-lines will have crossed the trace of the field boundary in which case olivine would now be undergoing resorption. As the trend of the projected curve LR (*cf.* trend of 1955 lavas, Fig. 8) is in the main away from the precipitated clinopyroxene neither voluminous precipitation of olivine, nor its strong resorption are to be expected in this range. This inference accords with petrographic observation and contrasts with the crystallization of plentiful groundmass olivine together with augite in more alkaline basalts such as one represented by point W. Unless fractionation is extreme hypersthene is not to be expected from a liquid X, and it is to be remembered that if fractionation were extreme, the Fe/Mg and albite/anorthite ratios may be so modified as to upset the basic form of the diagram shown.

From a liquid Y, representative of the Uwekahuna chilled magma and the Ascension Island hypersthene-bearing basalt referred to above, separation of

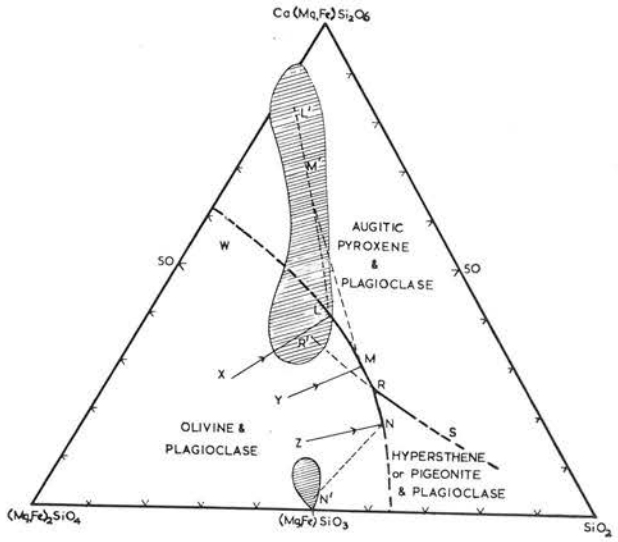

FIG. 9. Possible form of equilibrium relations for basaltic liquids within the olivine-pyroxene-silica-plagioclase tetrahedron, the floor of the plagioclase volume being projected from the plagioclase point onto the base of the tetrahedron. Composition fields of tholeiitic pyroxenes are shaded. Compositions are in molecular proportions.

olivine would yield accumulates comparable to the 1840 picrite basalt and the olivine-rich phases of the Uwekahuna mass, together with a liquid fraction reaching the augite-olivine boundary at M. Augite or subcalcic augite trending from M′ to R′ should then crystallize while the liquid moves from M to R. In the later stages of this process olivine is partly resorbed. At R, pigeonitic augite R′ should be joined by hypersthene or a related pigeonite and olivine would undergo continued resorptive reaction. The position of the five-phase point R is not fixed, but will migrate as this reaction proceeds as well as with other compositional changes and any pressure change. Fractionation of such a liquid by effective removal of olivine should lead to crystallization along a plagioclase-two pyroxene-liquid curve (RS), and the eventual appearance of free silica.

Separation of olivine from a liquid Z would displace it to the hypersthene or pigeonite field boundary at N where hypersthene (or pigeonite) should start to appear. The liquid should then move upwards along a curve such as NR as olivine is resorbed, hypersthene and olivine being joined at R by groundmass pigeonitic augite.

It will be noticed that for magmas with indicator ratios progressively smaller than the theoretical maximum of 1.00, the proportion of olivine resorbed to pyroxene crystallized becomes progressively smaller, in other words the Bowen reaction relationship becomes weaker. For indicator ratios somewhere near the middle of the range the reaction relationship disappears altogether and for lower values groundmass olivine can crystallize side by side with augitic pyroxene. For indicator ratios less than about 0.60 also, the appearance of hypersthene or pigeonite becomes progressively more unlikely and can only be achieved after increasingly strong fractionation.

Origin of Tholeiitic Magmas

It is noticeable that the compositions of the voluminous batches of typically tholeiitic magma plotted on Fig. 4, fall close to the inferred five-phase point olivine-augitic pyroxene-hypersthene-plagioclase-liquid of Fig. 9. In so far as the equilibria are not displaced by high pressure, partial fusion of a crystalline aggregate containing the solid phases mentioned would give rise to such liquids. This suggests a possible origin for tholeiitic magmas. Partial fusion of crystalline aggregates lacking hypersthene would be freed of this control.

As shown by Macdonald (1949b), Tilley (1960a) and others, the variation between the different variants of particular Kilauean eruptions may well be explained on the basis of crystal fractionation in upper crustal levels, the effects being clearly illustrated in Fig. 8. Differences in indicator ratio between such different batches of magma are much more difficult to account for on this basis. Increasing oxidation will slightly increase the indicator ratio and separation of pyroxene from liquids on the olivine-pyroxene-plagioclase-liquid curve will displace them towards tholeiitic composition if they fall initially within the diopside-olivine-plagioclase-silica tetrahedron, and probably towards more alkaline compositions if they contain substantial normative nepheline. The simplest interpretation of magma batches occupying intermediate positions in the basalt series of Fig. 4 (*e.g.* Réunion, Easter Island) is that these, like the more tholeiitic and alkaline extremes, may be true parental rather than derivative magmas. Yoder and Tilley (1961) and Kuno (1960) have indicated a possible mechanism that might bring this about.

Summary of Conclusions

(a) Averaged basalt analyses from various petrographic provinces plot across the normative Di-Ne-Ol-Qz diagram in a broad band. They range from typically tholeiitic suites with high indicator ratio $(Hy+2Qz)/Hy+2(Qz+Di)$, through transitional and mildly alkaline types with indicator ratio 0.40 to 0.00, to alkaline types with nepheline in the norm and in effect a negative indicator ratio. The first group gives rise to granophyric differentiates, at least some of the transitional group follow a pantelleritic trend the later stages of which cannot be properly represented in the tetrahedron here employed, whereas a phonolitic line of descent is followed by more strongly alkaline basalts. A trachytic trend appears to be characteristic of magmas with an indicator ratio near zero, that is, with neither significant normative nepheline nor hypersthene.

(b) Early crystallization of olivine and feldspar from most basaltic magmas may be considered to displace the liquid composition to an olivine-pyroxene-plagioclase boundary curve within the tetrahedron diopside-olivine-silica (or -nepheline).

(c) Clinopyroxenes are commonly strongly undersaturated in terms of normative components, the degree of undersaturation varying with that of the host rock. Clinopyroxene from alkaline basaltic rocks

usually contains normative nepheline and olivine, that from tholeiites, normative olivine and hypersthene.

(d) Except for liquid compositions falling close to the Pl-Di-Ol plane, separation of clinopyroxene will usually tend to offset the liquid away from that plane, either towards greater undersaturation if sufficient normative nepheline is originally present, or towards more silica-rich compositions if normative hypersthene or quartz is present.

(e) Detailed consideration of Hawaiian lavas and their pyroxenes suggests a five-phase, two-pyroxene reaction "point" on the olivine-pyroxene-plagioclase-liquid "curve" in the general region Di 26, Hy 54, Qz 20 in normative molecular proportions. In more approximate fashion this conclusion is compatible with the common behaviour of basaltic rocks in a substantial number of petrographic provinces.

(f) If the indicator ratio in a magma exceeds about 0.60 to 0.70 hypersthene or an equivalent pigeonite is likely to be the first pyroxene to commence to crystallize. If the ratio is between 0.50 and 0.65, a pyroxene trend from diopsidic pyroxene to subcalcic or pigeonitic augite may culminate in the subsequent appearance of a separate lime-poor phase. If the ratio is less than 0.50, hypersthene is unlikely to appear during the period of normal magmatic crystallization. The olivine-pyroxene reaction relationship progressively fades away for decreasing values of the indicator ratio and in many mildly alkaline rocks (low indicator ratio) olivine and augite crystallize simultaneously in comparable amounts.

References

Andersen, O. (1915) The system anorthite-forsterite-silica. *Am. Jour. Sci.* 4th ser., **39,** 407–454.

Anderson, C. A. (1941) Volcanoes of the Medicine Lake Highland, California. *Bull. Dept. Geol. Sci., Univ. Calif. Publ.* **25,** 347–422.

Bandy, M. C. (1937) Geology and petrology of Easter Island. *Geol. Soc. Am. Bull.* **48,** 1589–1610.

Benson, W. N. (1941) Cainozoic petrographic provinces in New Zealand and their residual magmas. *Am. Jour. Sci.* **239,** 537–552.

——— (1942) The basic igneous rocks of Eastern Otago and their tectonic environment. Part II. *Trans. Roy. Soc. New Zealand,* **72,** 85–110.

Bowen, N. L. (1914) The ternary system diopside-forsterite-silica. *Am. Jour. Sci.* 4th ser., **38,** 207–264.

——— and J. F. Schairer (1935) The system MgO-FeO-SiO_2. *Am. Jour. Sci.* ser 5, **29,** 151–217.

Boyd, F. R. and J. F. Schairer (1957) The join $MgSiO_3$-$CaMgSi_2O_6$. *Carnegie Inst. Washington Year Book,* **56,** 223–225.

Brown, G. M. (1957) Pyroxenes from the early and middle stages of fractionation of the Skaergaard intrusion, East Greenland. *Mineral. Mag.* **31,** 511–543.

——— (1960) The effect of ion substitution on the unit cell dimensions of the common clinopyroxenes. *Am. Mineral.* **45,** 15–38.

Cornwall, H. R. (1951) Differentiation in magmas of the Keweenawan series. *Jour. Geol.* **59,** 151–172.

Daly, R. A. (1924) The geology of American Samoa. *Carnegie Inst. Papers Dept. Marine Biol.* **19,** 93–143.

——— (1925) The geology of Ascension Island. *Proc. Am. Acad. Arts Sci.* **60,** (1).

——— (1927) The geology of Saint Helena Island. *Proc. Am. Acad. Arts Sci.* **62,** 31–92.

Edwards, A. B. (1938) Tertiary tholeiite magma in western Australia. *Jour. Roy. Soc. West. Austr.* **24,** 1–12.

——— (1942) Differentiation of the dolerites of Tasmania. *Jour. Geol.* **50,** 451–480, 579–610.

Fairbairn, H. W. and others (1951) A cooperative investigation of precision and accuracy in chemical, spectrochemical and modal analysis of silicate rocks. *U. S. Geol. Surv. Bull.* **980.**

Green, J. and A. Poldervaart (1955) Some basaltic provinces. *Geochim. Cosmochim. Acta,* **7,** 177–188.

Gunn, B. M. (1962) Differentiation in Ferrar Dolerites, Antarctica. Ph.D. thesis, University of Otago.

Harkin, D. A. (1960) The Rungwe volcanics at the northern end of Lake Nyasa. *Geol. Surv. Tanganyika Mem.* **2.**

Hess, H. H. (1960) Stillwater igneous complex, Montana. *Geol. Soc. Am. Mem.* **80.**

Hytönen, K. and F. J. Schairer (1960) The system enstatite-anorthite-diopside. *Carn. Inst. Washington Year Book* 1959–60, 71–72.

Jung, D. (1958) Untersuchungen am Tholeyit von Tholey (Saar). *Beitr. Mineral. Pet.* **6,** 147–181.

Kuno, H. (1950) Petrology of Hakone volcano and the adjacent areas, Japan. *Geol. Soc. Am. Bull.* **61,** 957–1020.

——— (1955) Ion substitution in the diopside-ferropigeonite series of clinopyroxenes. *Am. Mineral.* **40,** 70–93.

——— (1960) High-alumina basalt. *Jour. Petrol.* **1,** 121–145.

——— K. Yamasaki, C. Iida and K. Nagashima (1957) Differentiation of Hawaiian magmas. *Jap. Jour. Geol. Geog.* **28,** 179–218.

LaCroix, A. (1927) La constitution lithologique des îles volcaniques de la Polynésie australe. *Acad. Sci. Paris, Mem.* **59,** 1–82.

——— (1936) *Le volcan actif de l'île de la Réunion et ses produits.* Paris, Gauthier-Villars.

Macdonald, G. A. (1949a) Petrography of the Island of Hawaii. *U. S. Geol. Surv. Prof. Paper,* **214D,** 1–96.

——— (1949b) Hawaiian petrographic province. *Geol. Soc. Am. Bull.* **60,** 1541–1596.

——— (1955) *Catalogue of the active volcanoes of the world. Part III. Hawaiian Islands.* Naples Intl. Volcan. Assoc., 35–36.

——— and J. P. Eaton (1955) Hawaiian volcanoes during 1953. *U. S. Geol. Surv. Bull.* **1021-D,** 160.

Muir, I. D. (1951) The clinopyroxenes of the Skaergaard intrusion, eastern Greenland. *Mineral. Mag.* **29,** 690–714.

——— AND C. E. TILLEY (1957) Contributions to the petrology of Hawaiian basalts. I. The picrite basalts of Kilauea. *Am. Jour. Sci.* **255,** 241–253.

——— C. E. TILLEY AND J. H. SCOON (1961) Mugearites and their place in alkali igneous rock series. *Jour. Geol.* **69,** 186–203.

MURATA, K. J. (1960) A new method of plotting chemical analyses of basaltic rocks. *Am. Jour. Sci.* **258-A,** 247–252.

——— AND D. H. RICHTER (1961) Magmatic differentiation in the Uwekahuna Laccolith, Kileauea Caldera, Hawaii. *Jour. Petrol.* **2,** 427–437.

MURRAY, R. J. (1954) The clinopyroxenes of the Garbh Eilean Sill, Shiant Isles. *Geol. Mag.* **91,** 17–31.

NAIDU, P. R. J. (1960) Optic axial angles of pyroxenes of Deccan Traps. *Indian Mineral.* **1,** 68–75.

OSBORN, E. F., AND A. MUAN (1960) *Phase equilibrium diagrams of oxide systems.* Am. Ceram. Soc.

——— AND D. B. TAIT (1952) The system diopside-forsterite-anorthite. *Am. Jour. Sci. Bowen vol.* 413–433.

RICHARDSON, C. (1933) Petrology of Galapagos Islands. *Bernice P. Bishop Museum Bull.* **110,** 45–64.

ROSS, C. S., M. D. FOSTER AND A. T. MYERS (1954) Origin of dunites and of olivine-rich inclusions in basaltic rocks. *Am. Mineral.* **39,** 693–737.

SCHAIRER, J. F. AND N. MORIMOTO (1959) The system forsterite-diopside-silica-albite. *Carn. Inst. Washington Year Book,* **58,** 113–118.

——— AND H. S. YODER (1960) The system olbite-forsterite-silica. *Carn. Inst. Washington Year Book,* **59,** 69–70.

SEARLE, E. J. (1960) Petrochemistry of the Auckland basalts. *New Zealand Jour. Geol. Geophys.* **3,** 23–40.

SPEIGHT, R. (1938). The dykes of the Summit Road, Lyttleton. *Trans. Roy. Soc. New Zealand* **68,** 82–99.

SUKHESWALA, R. N. AND A. POLDERVAART (1958) Deccan basalts of the Bombay area, India. *Geol. Soc. Am. Bull.* **69,** 1475–1494.

TILLEY, C. E. (1950) Some aspects of magmatic evolution. *Quart. Jour. Geol. Soc. London,* **106,** 37–61.

——— (1960a) Differentiation of Hawaiian basalts: some variants in lava suites of dated Kilauean eruptions. *Jour. Petrol.* **1,** 47–55.

——— (1960b) Kilauea magma, 1959–60. *Geol. Mag.* **97,** 494–497.

——— (1961) The occurrence of hypersthene in Hawaiian basalts. *Geol. Mag.* **98,** 257–260.

——— AND J. H. SCOON (1961) Differentiation of Hawaiian basalts: trends of Mauna Loa and Kilauea historic magma. *Am. Jour. Sci.* **259,** 60–68.

TRYGGVASON, T. (1943) Das Skjaldbreid-Gebiet auf Island. *Bull. Geol. Inst. Upsala,* **30,** 273–320.

WAGER, L. R. (1960) The major element variation of the layered series of the Skaergaard intrusion and a re-estimation of the average compositions of the hidden layered series and of the successive residual magmas. *Jour. Petrol.* **1,** 364–398.

——— AND W. A. DEER (1939) The petrology of the Skaergaard Intrusion, Kangerdlugssuak, East Greenland. *Medd. om. Grønland,* **105.**

WALKER, F. (1940) Differentiation of the Palisade diabase, New Jersey. *Geol. Soc. Am. Bull.,* **51,** 1059–1106.

——— AND NICOLAYSEN, L. O. (1954) The petrology of Mauritius. *Col. Geol. Min. Res.* **4,** 3–43.

——— AND POLDERVAART, A. (1949) Karroo dolerites of the Union of South Africa. *Geol. Soc. Am. Bull.* **60,** 591–706.

WATERS, A. C. (1961) Stratigraphic and lithologic variations in the Columbia River basalt. *Am. Jour. Sci.* **259,** 583–611.

WENTWORTH, C. K. AND H. WINCHELL (1947) Koolau basalt series, Oahu, Hawaii. *Geol. Soc. Am. Bull.* **58,** 49–78.

WEST, W. D. (1958) The petrography and petrogenesis of forty-eight flows of Deccan trap penetrated by borings in western India. *Trans. Nat. Inst. Sci. India.* **IV** (1), 1–56.

WILKINSON, J. F. G. (1957) The clinopyroxenes of a differentiated teschenite sill near Gunnedah, New South Wales. *Geol. Mag.* **94,** 123–134.

——— (1958) The petrology of a differentiated teschenite sill near Gunnedah, New South Wales. *Am. Jour. Sci.* **256,** 1–39.

WILLIAMS, H. (1933) Geology of Tahiti, Moorea, and Maiao. *Bernice P. Bishop Museum Bull.* **105.**

WINCHELL, H. (1947) Honolulu series, Oahu, Hawaii. *Geol. Sco. Am. Bull.* **58,** 1–48.

YAGI, K. (1953) Petrochemical studies of the alkali rocks of the Morotu district, Sakhalin. *Geol. Soc. Am. Bull.* **64,** 769–810.

YODER, H. S. AND C. E. TILLEY (1957) Basalt magmas. *Carn. Inst. Washington Year Book,* **56,** 156–161.

——— AND C. E. TILLEY (1960) Simple basalt systems. *Carn. Inst. Washington Year Book,* **59,** 67–69.